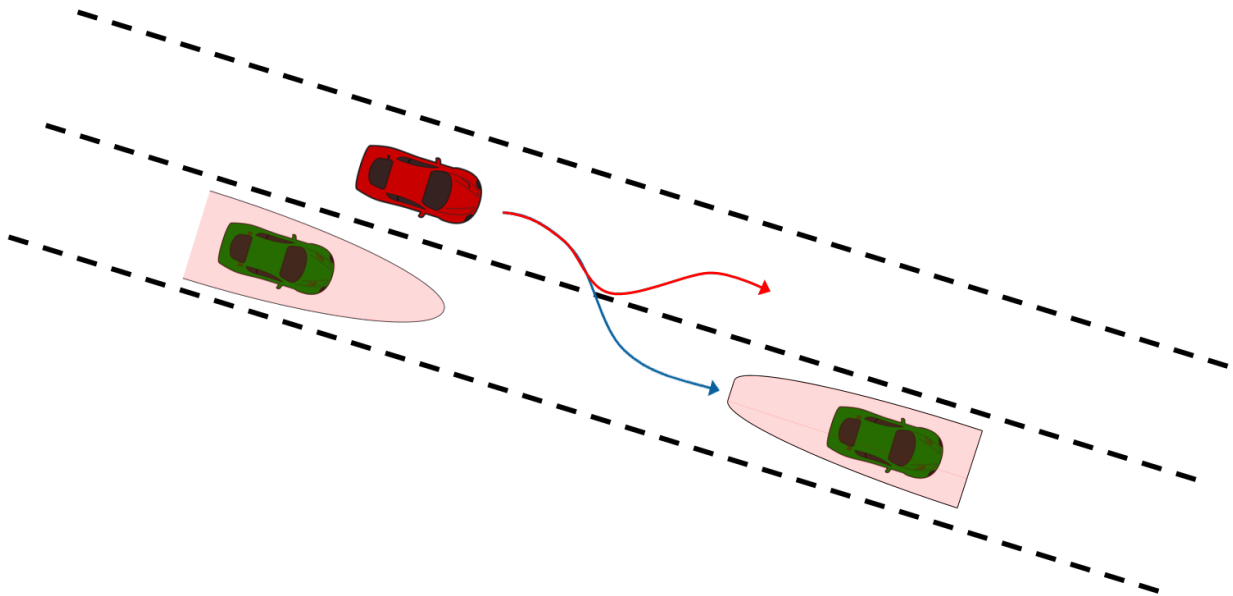




**CHALMERS**  
UNIVERSITY OF TECHNOLOGY

---



# Motion Planning for Autonomous Lane Change Manoeuvre with Abort Ability

Master's thesis in Systems, Control and Mechatronics

Rajashekar Chandru  
Yuvaraj Selvaraj



MASTER'S THESIS 2016:EX055

# Motion Planning for Autonomous Lane Change Manoeuvre with Abort Ability

Rajashekar Chandru  
Yuvaraj Selvaraj



Department of Signals and Systems  
*Division of Automatic Control, Automation and Mechatronics*  
Mechatronics research group  
CHALMERS UNIVERSITY OF TECHNOLOGY  
Gothenburg, Sweden 2016

Motion Planning for Autonomous Lane Change Manoeuvre with Abort Ability  
RAJASHEKAR CHANDRU  
YUVARAJ SELVARAJ

© RAJASHEKAR CHANDRU, YUVARAJ SELVARAJ, 2016.

Supervisor: Roozbeh Kianfar, Volvo Cars Corporation  
Supervisor: Mattias Brännström, Volvo Cars Corporation  
Examiner: Nikolce Murgovski, Signals and Systems

Master's Thesis 2016:EX055  
Department of Signals and Systems  
Division of Automatic Control, Automation and Mechatronics  
Mechatronics research group  
Chalmers University of Technology  
SE-412 96 Gothenburg  
Telephone +46 31 772 1000

Cover: Illustration of a motion planned for lane change manoeuvre with the ability to abort.

Typeset in L<sup>A</sup>T<sub>E</sub>X  
Printed by Chalmers Reproservice  
Gothenburg, Sweden 2016

Motion Planning for Autonomous Lane Change Manoeuvre with Abort Ability  
RAJASHEKAR CHANDRU  
YUVARAJ SELVARAJ  
Department of Signals and Systems  
Chalmers University of Technology

## Abstract

The field of highly autonomous ground vehicle systems has been the focus of research in both, academia and industry in the recent decades and is expected to be so in the near future. The work in this thesis focuses on one aspect of highly autonomous vehicles - motion planning in complex traffic environments. The scope of this thesis is limited to motion planning for autonomous lane change and lane change abortion manoeuvres in dense urban traffic scenarios. The purpose of the work is to tackle the problem of autonomous lane change driving in uncertain traffic environments where the vehicle has to anticipate and adapt to behaviour of the surrounding vehicles. The solution is presented as a robust algorithm which is tolerant to uncertainties in the planning horizon. Safety is guaranteed by modelling the safety critical areas around the surrounding vehicles which the autonomous vehicle should not enter in order to plan an evasive action. The problem of motion planning during the entire manoeuvre is solved as two loosely coupled problems. A longitudinal trajectory is first planned and then for a given longitudinal trajectory, the lateral motion is planned with respect to the safety constraints using Model Predictive Control (MPC). The proposed solution is then evaluated for a series of scenarios in a simulation environment modelled using MATLAB/Simulink. Different unexpected behaviours of the surrounding vehicles are simulated and the results show that the proposed algorithm is capable of handling the simulated scenarios. The thesis is concluded with discussions on the results and possible future extension of the work carried out in this thesis.

Keywords: motion planning, Model Predictive Control, Autonomous vehicles, collision avoidance, backup path, lane change control, lane change abortion.



# Acknowledgements

The work in this thesis was carried out in close collaboration with Volvo Cars Corporation and we are thankful for giving us the opportunity to work on such an exciting problem. It has been an interesting and enjoyable journey and a number of people have to be credited for the same. Firstly, we would like to thank our supervisors, Mattias Brännström and Roozbeh Kianfar at Volvo Cars Corporation for their interest and guidance throughout the project. We enjoyed our discussions as much as we enjoyed the work and we would like to thank them for asking us the right questions all along the way which helped us refine our work in a better way.

We are very grateful to our examiner, Assistant Professor Nikolce Murgovski at Chalmers who has provided valuable insights through critical questioning on both our work in the thesis and also on the presentation and documentation of our results. We thank him for giving us his time whenever we required.

A special acknowledgement goes to Mohsen Nosratinia at Volvo Cars Corporation for letting us use his work in our thesis and also for answering our questions related to that.

Finally, we would also like to thank our colleagues at Volvo Car Corporation for giving us a very comfortable and inspiring work environment. We have acquired valuable knowledge through all the Group Technical Meetings and we are grateful for giving us the opportunity to be a part of it.

Rajashekhar Chandru, Yuvaraj Selvaraj, Gothenburg, June 2016



# Contents

<b>List of Figures</b>	<b>xi</b>
<b>List of Tables</b>	<b>xv</b>
<b>1 Introduction</b>	<b>1</b>
1.1 Problem background . . . . .	1
1.2 Purpose . . . . .	3
1.3 Scope . . . . .	4
1.4 Related work . . . . .	4
1.5 Scientific Contributions . . . . .	5
1.6 Outline . . . . .	5
<b>2 Problem Description &amp; Relevant Theory</b>	<b>7</b>
2.1 Theoretical preliminaries and definitions . . . . .	7
2.2 Problem description . . . . .	9
2.3 Vehicle model . . . . .	10
2.3.1 Point mass vehicle model . . . . .	11
<b>3 Methods</b>	<b>13</b>
3.1 Critical zone . . . . .	13
3.1.1 Assumptions in critical zone modelling . . . . .	13
3.1.2 Acceleration profiles . . . . .	14
3.1.2.1 Determining lateral acceleration profile for a fixed lane width . . . . .	15
3.1.3 Leading vehicles in adjacent lane . . . . .	17
3.1.4 Trailing vehicles in adjacent lane . . . . .	19
3.1.5 Vehicles in host lane . . . . .	20
3.2 Desired final position . . . . .	22
3.3 Longitudinal motion planning . . . . .	23
3.4 Lateral motion planning . . . . .	26
<b>4 Results</b>	<b>29</b>
4.1 Part A . . . . .	29
4.1.1 Critical Zone . . . . .	30
4.1.2 Improvements in lane change efficiency . . . . .	31
4.1.3 Desired Final Position . . . . .	32
4.1.4 Longitudinal Motion Planning . . . . .	33

4.1.5	Lateral Motion Planning . . . . .	34
4.1.6	Simulation of the planned trajectory . . . . .	36
4.2	Part B . . . . .	37
4.2.1	Case 1 - Ego vehicle steers to avoid collision . . . . .	37
4.2.2	Case 2 - Ego vehicle brakes to avoid collision . . . . .	40
4.2.3	Case 3 - Ego vehicle plans a new path to get back to host lane . . . . .	41
<b>5</b>	<b>Discussions</b>	<b>45</b>
5.1	Performance with different assumptions about surrounding vehicles . . . . .	45
5.2	Different motion models . . . . .	46
5.2.1	Bicycle model . . . . .	46
5.2.2	Comparison of different vehicle models in critical zone modelling . . . . .	48
5.3	Analytical solutions for motion planning . . . . .	48
<b>6</b>	<b>Conclusion</b>	<b>51</b>
6.1	Future work . . . . .	52
	<b>Bibliography</b>	<b>53</b>

# List of Figures

2.1	Lateral offset between the two vehicles. The ego vehicle is shown in red and the leading vehicle is shown in green. . . . .	8
2.2	Time gap between two vehicles. The ego vehicle depicted in red has $X_{Initial}$ as the longitudinal position with velocity $V_{Initial}$ . The leading vehicle depicted in green in front of it has the position $X_{Final}$ . . . . .	9
2.3	Traffic scenario with vehicles travelling in two lanes. Ego vehicle is shown in red. T1 and T2 are trailing vehicles. L1 and L2 are leading vehicles. Shaded area depicted by red colour is the critical zone. . . . .	10
3.1	The longitudinal acceleration profile for braking. The ego vehicle is modelled to follow a constant jerk profile until time $t_0$ , where it reaches the maximum deceleration limit, $a_x^{max}$ . The vehicle follows a constant acceleration profile from time $t_0$ to final time $t_f$ . . . . .	14
3.2	The lateral acceleration profile for steering. The ego vehicle is modelled to follow a constant jerk profile until time $t_0$ , where it reaches the maximum acceleration $a_y^{max}$ . The ego vehicle follows a constant acceleration profile from time $t_0$ to $t_1$ . From $t_1$ to $t_2$ , it follows a deceleration profile with constant jerk until zero acceleration is achieved. Constant zero acceleration is maintained from time $t_2$ to final time $t_f$ . . . . .	15
3.3	Complete acceleration profile for steering evasive manoeuvre. The black curve indicates the evasive steering from the target lane for the ego vehicle to avoid collision and the red curve indicates the ego vehicle's manoeuvre back into the host lane. . . . .	16
3.4	Critical zone calculation for the leading vehicle when the ego vehicle brakes to avoid a collision. Ego vehicle denoted by E is represented in red colour and the leading vehicle denoted by L is depicted in green colour. . . . .	18
3.5	Critical zone calculation for the leading vehicle when the ego vehicle steers to avoid a collision. Ego vehicle denoted by E is represented in red colour and the leading vehicle denoted by L is depicted in green colour. . . . .	19
3.6	Critical time calculation for trailing vehicle in adjacent lane. $S_{latsafe}$ is the minimum distance required to travel for the ego vehicle E to avoid a collision with the trailing vehicle T. The dotted line represent the safe width limit and the thick line denote the lane limits. . . . .	20

3.7	Critical time calculation for leading vehicle in host lane. $S_{\text{leading}}$ and $S_{\text{ego}}$ being the braking distance travelled by the leading vehicle L and ego vehicle E respectively. The dotted line represents the lane centres and the thick line denotes the lane limits. . . . .	21
3.8	Critical time calculation for trailing vehicle in host lane. $S_{\text{trailing}}$ and $S_{\text{ego}}$ being the braking distance travelled by the trailing vehicle T and ego vehicle E respectively. The dotted line represents the lane centres and the thick line denotes the lane limits. . . . .	22
3.9	Scenario where the ego vehicle can manoeuvre into the centre of the target lane. The predicted final positions of the leading and trailing vehicle at the end of lane change time, with their critical zones are shown. The blue line represents the trajectory of the ego vehicle, during the lane change. . . . .	23
3.10	Scenario where ego vehicle positions itself at the intersection of the critical zones of surrounding vehicle at the end of the lane change time. The predicted final positions of the leading and trailing vehicle at the end of lane change time, with their critical zones are shown. The blue line represents the trajectory of the ego vehicle, during the lane change. . . . .	23
4.1	Critical zones plotted for the initial positions of all occupants in the traffic environment as mentioned in Table 4.1. Ego vehicle, depicted with a red star in the centre, is the only occupant in the initial host lane. The critical zones are predicted with respect to the shown position of the ego vehicle. . . . .	30
4.2	Lateral and Longitudinal acceleration profiles considered to calculate the critical zone as explained in Section 3.1. <i>Left</i> : Lateral acceleration profile considered for the ego vehicle to plan the evasive action by steering. <i>Right</i> : Longitudinal deceleration profile considered for the ego vehicle to plan the evasive action by braking. . . . .	30
4.3	The lateral intrusion by the critical edge of the ego vehicle into the target lane is plotted against the time gap between the trailing and leading vehicle in adjacent lane. The current assumption is that the lead vehicle can come to crash stop at any instance, and that the trailing vehicle accelerates in order to cut off the lane change manoeuvre. The results are plotted for velocities of ego, trailing and leading vehicle as 18 m/s. . . . .	31
4.4	The lateral intrusion by the critical edge of the ego vehicle into the target lane is plotted against target lane velocity for different time gaps. Both the leading and trailing vehicles in the target lane maintain the same target lane velocity. . . . .	32
4.5	Desired final position for the ego vehicle calculated based on the intersection of the predicted critical zones at the end of the lane change time. . . . .	33
4.6	Longitudinal Position of the ego vehicle planned over the entire lane change time of 5 seconds. . . . .	33

4.7	<i>Left:</i> Velocity profile of the ego vehicle for the planned longitudinal motion with an initial velocity of 16 m/s and final desired velocity of 18m/s. <i>Right:</i> Acceleration profile of the ego vehicle for the planned longitudinal motion with an initial and final desired value of 0m/s <sup>2</sup> . . . . .	34
4.8	Lateral Position of the ego vehicle planned over the entire lane change time of 5 seconds. . . . .	34
4.9	<i>Left:</i> Velocity profile of the ego vehicle for the planned lateral motion. <i>Right:</i> Acceleration profile of the ego vehicle for the planned lateral motion. . . . .	35
4.10	Simulation of the proposed motion planning algorithm in a traffic scenario where ego vehicle has to leave its host lane and position itself in the adjacent lane between the two surrounding vehicles. . . . .	36
4.11	<i>Scenario 1:</i> Lane change scenario where the leading vehicle comes to an immediate stop at the end of lane change time. The ego vehicle steers away to avoid collision with the leading vehicle. . . . .	38
4.12	Longitudinal and Lateral velocity and acceleration profile of the Ego vehicle in <i>Scenario 1</i> . In this scenario, the ego vehicle steers away to avoid a collision. . . . .	39
4.13	<i>Scenario 2:</i> Lane change scenario where the trailing vehicle accelerates with a constant acceleration of 2 m/s <sup>2</sup> at the end of lane change time. The ego vehicle steers away to avoid collision. . . . .	40
4.14	<i>Scenario 3:</i> Lane change scenario where the leading vehicle comes to an immediate stop at the end of lane change time. The ego vehicle brakes to avoid collision with the leading vehicle. . . . .	41
4.15	<i>Top:</i> Longitudinal velocity profile of the ego vehicle in <i>Scenario 3</i> . <i>Bottom:</i> Longitudinal acceleration profile of the ego vehicle in <i>Scenario 3</i> . . . . .	42
4.16	<i>Scenario 4:</i> Lane change scenario where the trailing vehicle accelerates during the ego vehicle's lane change manoeuvre. The algorithm is used to generate a new motion plan for the ego vehicle to get back to the initial host lane. . . . .	43
4.17	Longitudinal and Lateral velocity and acceleration profile of the Ego vehicle in <i>Scenario 4</i> . In this scenario, the behaviour of the surrounding vehicles does not match the assumptions used for path prediction. . . . .	44
5.1	The lateral intrusion by the critical edge of the ego vehicle into the target lane is plotted against the time gap between the trailing and leading vehicle in adjacent lane. The blue curve shows the gain with the current assumption and the red curve shows the gain with the change in assumptions about the surrounding vehicles. The results are plotted for velocities of ego, trailing and leading vehicle as 18 m/s. . . . .	46
5.2	Single-track model, showing the combined front and rear tire forces, the steering angle $\delta$ , the yaw rate $\dot{\psi}$ , and the vehicle side-slip angle $\beta$ . . . . .	47
5.3	Critical time gap plotted as a function of offset in the target lane for both pointmass and bicycle model . . . . .	48



# List of Tables

3.1	Steps to calculate the intersection point of the critical zones around the predicted final positions of the leading and trailing vehicles. . . .	24
3.2	Steps to determine the lateral constraints over the prediction horizon	27
4.1	General simulation parameters for the lane change scenario with a lane change time of 5 seconds and a desired final ego velocity of 18 (m/s) . . . . .	29
4.2	General parameters for the lane change scenario with a lane change time of 5 seconds and a desired final ego velocity of 18 (m/s) . . . . .	38



# 1

## Introduction

The World Health Organisation reports that more than 1.2 million people die each year due to road traffic injuries. This makes road traffic accidents a leading cause of human death globally [2]. The National Highway Traffic Safety Administration of the United States, estimated the number of people injured in road accidents in 2014 to be 2.34 million [5]. About 58 percent of traffic accidents causing deaths in Sweden in the recent years were in a car and about 36 percent of these accidents were vehicle to vehicle collision [6]. The total cost for road traffic accidents that occurred in Sweden in 2005 was reported to be €2.25 billion in 2005 prices [3]. The total economic cost of traffic crashes was estimated at around €5.2 billion in 2011 [4]. In 2010, a total economic cost of \$242 billion was reported due to motor vehicle crashes in the United States [7]. There is extensive literature available on the potential benefits of Autonomous Driving (AD) and Advanced Driver Assistance Systems (ADAS) with the most important being reducing the number of human traffic deaths [8] [9] [10]. Some of the potential benefits include reduction in traffic accidents, increased safety, significant driver experience, fuel savings and pollution reduction benefits.

Autonomous Driving has been one of the main focus of research in academia and within the automotive industry in the recent years and will continue to be so in a foreseeable future. Automotive manufacturers are moving more and more towards ground vehicle autonomy on different levels. Several advanced driver assistance functions like Adaptive Cruise Control (ACC), emergency Lane Keeping Assist (eLKA), parking assist and collision avoidance systems are already in production and becoming standard in the recent years.

### 1.1 Problem background

The Society of Automotive Engineers (SAE) International defines vehicle automation to have six levels from no automation to full automation[11]. These levels are found to be useful in benchmarking and examining the different types of technologies:

- No Automation (Level 0): The driver is in complete control of all driving aspects of the vehicle.
- Driver Assistance (Level 1): One or more driving mode specific control func-

tions like cruise control, auto braking, and lane keeping. Execution of steering, acceleration and deceleration performed by the system are expected to assist the human driver.

- Partial Automation (Level 2): At least two driving mode specific control functions working together to assist the driver. An example of this level is adaptive cruise control with lane centring.
- Conditional Automation (Level 3): Automated driving system performs driving mode specific functions with the expectation that the human driver will respond to an intervention request.
- High Automation (Level 4): Automated driving system performs all driving mode specific functions even if the human driver does not respond to an intervention request.
- Full Automation (Level 5): Full time automated performance of all driving functions of the vehicle

Although most of the vehicles in production today are within the first two defined levels, Level 2 and 3 are being introduced by some manufacturers and vehicle autonomy at higher levels are at experimental stages. A lot of focus in research has been fuelled towards Level 4 and Level 5 vehicles and the road to achieving full autonomy is not devoid of technological and social challenges. Several research projects are in existence today, where experts from academia and from the industry work closely to tackle these challenges. Some of the notable projects being the Defence Advanced Research Projects Agency (DARPA) challenges and the Grand Cooperative Driving Challenge (GCDC). Technology leaders like Volvo, BMW and Google among others have currently tested for certain levels of autonomy and also have planned for experimental tests and production of various levels of autonomous vehicles in the future [13] [14].

Significant research has been done in what is perceived as the most difficult challenges in the development of autonomous vehicles - the areas of sensor perception and decision making under uncertain conditions [15]. Fully autonomous vehicles (Level 4) should be able to control all safety critical functions without driver supervision under all operating conditions, which includes different traffic environments like structured highway traffic and dense urban traffic conditions among others. Under complex traffic environments, which consists of different players like independently operating surrounding vehicles, dynamic obstacles (animals, pedestrians, etc.), and unexpected emergencies like construction site, emergency vehicles (ambulances, fire engines) and crashes, it is a challenging task for the autonomous vehicle to execute safe behaviours without affecting the environment. Specifically, tasks like lane changing and overtaking autonomously becomes challenging because it is difficult for the autonomous vehicle to understand and anticipate the intentions of the other vehicles and users.

Motion planning is a key function in development of autonomous vehicles. Ensuring safe autonomous manoeuvres like overtaking and lane changing is a vital part towards development of this technology. The vehicle must be able to manoeuvre from

the starting point to the desired destination safely and also be tolerant to prediction errors over the planning horizon. To navigate in complex traffic scenarios like dense urban traffic, the autonomous vehicle must be able to change lanes as often as it wants to without risking safety. Having a backup motion plan in such conditions is important to ensure a safe operation and also improve tolerance to uncertainties. This thesis focuses on motion planning for autonomous vehicles during lane change and lane change abortion manoeuvres. This thesis will be connected to Volvo's unique pilot, where Volvo plans to lease 100 self-driving vehicles to real customers. The vehicles will be capable of driving autonomously around the city of Gothenburg without requiring driver supervision [16].

## 1.2 Purpose

The problem of generating a path for the autonomous vehicles to follow during lane change manoeuvres in a complex traffic scenario like dense urban traffic is a challenge that needs to be addressed. Availability of a motion plan for lane change abortion during such manoeuvres can make the autonomous vehicle accommodate large prediction errors. Very little research has been done which looks into backup motion planning in case of emergencies in complex traffic environments or in case of planned path abortion scenarios. Having a backup motion plan will also relax the constraints on lane change path generation, while guaranteeing the safe operation of the autonomous vehicle. This gives the autonomous vehicles the flexibility and confidence to initiate lane change manoeuvres more often which is the case with dense urban traffic scenarios. The presented thesis work focuses on the motion planning problem specific to lane change and lane change abortion scenarios.

The work done in the thesis project shall involve:

- **Improving the motion planning during lane change manoeuvres to be implementable in dense urban traffic scenarios.**

A suitable method will be proposed that will relax the constraints on the initiation and execution of lane change manoeuvres in complex environments like dense urban traffic scenarios.

- **Feasible**

The proposed algorithm shall guarantee feasibility, i.e., the paths planned should be within the physical (kinematic) limits of the vehicle and must be possible for the vehicle to follow.

- **Robust and Safe**

The proposed algorithm shall guarantee safety (collision free from surrounding vehicles) and be tolerant to accommodate prediction errors in the behaviour of the surrounding vehicles during the planning horizon.

- **Evaluation**

The results of the proposed algorithm are validated in a simulation environment (MATLAB/Simulink). Results are then followed with discussions.

The first phase of this work comprises a literature study on the related work done within this area. The next phase of the work involves the development of an algorithm for motion planning specific to lane change and lane change abortion in urban traffic scenarios. Finally different scenarios are simulated to evaluate the performance of the proposed algorithm.

### 1.3 Scope

The work done on this project is based on the following assumptions:

- The presence of a good environment sensing and perception system. A sensor system that provides a good representation of the environment including the positions of all vehicles and other required parameters within the mapped environment throughout the planning horizon is considered available.
- The presence of a control system to follow the planned path. In other words, the development of a path following controller is not within the scope of this thesis.
- The availability of a supervisory module to decide ideal conditions for initiation of lane change execution. Decision making on when to initiate the lane change manoeuvre is not investigated in this thesis.
- Lateral position of the surrounding vehicles is assumed to be constant throughout the planning, i.e., no lateral motion behaviour is assumed for the vehicles.
- The simulation results of the proposed algorithm does not include vehicles and other objects in the initial lane.

### 1.4 Related work

This section presents the literature study that was done during the initial phase of this thesis work. A comparative study of the different path planning methods and recommendations for future work is done in [17]. A survey on motion prediction and risk assessment for intelligent vehicles is discussed in [19]. In [18], given a particular lane change/merge scenario, a method to calculate the minimum longitudinal spacing which the vehicles should have is presented. It is also shown that this spacing is required to guarantee that no collision of any type takes place during the manoeuvre. Literature study involving optimal control for active safety of vehicles using steering and braking was also done. Model based threat assessment and decision making for collision avoidance in autonomous vehicles by steering, braking or accelerating is discussed in [27]. Computationally simple control algorithm for lane change is discussed in [28]. Predictive control for overtaking is discussed in [29], where a method for formulating the overtaking problem as a convex optimisation is also proposed.

## 1.5 Scientific Contributions

This thesis presents a novel method to assess the critical level of traffic situations. A method is proposed where the autonomous vehicle can make use of the ability to either brake or steer to avoid collisions. The method uses physical motion models to calculate a critical parameter to assess the safety, which is then used in the proposed motion planning algorithm. Secondly, a straightforward way of calculating the safest position in the target lane to complete the lane change manoeuvre is proposed. This method can be used to plan for manoeuvres where the autonomous vehicles are required to squeeze into tight gaps in complex traffic environments. Finally, a motion planning algorithm is proposed to perform autonomous lane change manoeuvres with the ability to abort the manoeuvre at any point with guaranteed safety. The motion planning algorithm is formulated and solved as decoupled longitudinal motion planning and lateral motion planning resulting from the solution of a Model Predictive Control (MPC) problem.

## 1.6 Outline

The next chapter in the thesis introduces the readers to the problem formulation and then provides some relevant background theory. Chapter 3 elaborates on the methods and the solutions used to plan a safe motion during lane change and lane change abortion. Evaluation of the proposed algorithm with simulation results and discussions on the proposed methods are presented in Chapter 4. The chapter also includes different scenarios that are simulated to evaluate the proposed algorithm. The final chapter presents the conclusions and recommendations for future work.



# 2

## Problem Description & Relevant Theory

This chapter first introduces the definitions of the important terms used in the context of this thesis to formulate and solve the problem. The second section presents the problem formulation of motion planning for autonomous lane change manoeuvres specific to the work in this thesis. The last section includes an explanation of the vehicle models which are used to model and solve the problem described.

### 2.1 Theoretical preliminaries and definitions

**Definition 1** *Ego vehicle in the context of this thesis is defined as the autonomous vehicle to be controlled.*

**Definition 2** *Trajectory is defined as a continuous curve connecting two points represented by a sequence of vehicle states. The vehicle states are usually considered to be a function of time.*

Trajectory planning (also known as motion planning) concerns with the real-time planning of the vehicle's motion from one state to another next state. The motion planning is usually done by ensuring that the vehicle's states are feasible with respect to different constraints. The constraints may be defined based on:

- the physical (actuator) limits of the vehicle or kinematic limits based on the dynamics of the vehicle.
- driving comfort of the vehicle. One widely used parameter to define parameter comfort is the rate of change of vehicle acceleration.
- safe driving conditions like staying within lane boundaries, avoiding obstacles in the traffic environment.

Trajectory planning or motion planning is more commonly parametrised by time while some cases where it is parametrised using velocity and acceleration can also be found in literature.

**Definition 3** *Time To Collision (TTC) is defined as the time left to collision if two vehicles continue on the same course with a constant velocity.*

TTC is a useful measure in assessing the critical level of a traffic situation and is a

## 2. Problem Description & Relevant Theory

commonly used safety indicator in collision avoidance and driver assistance systems. A low value of TTC indicates that a collision is bound to occur if none of the vehicles initiate any evasive action. In [22], TTC is also defined as the time that is needed to cover the distance between the lead and the following vehicle with the relative speed between the lead and the following vehicle and is computed as:

$$TTC_i = \frac{X_{i-1}(t) - X_i(t) - l_i}{\dot{X}_i(t) - \dot{X}_{i-1}(t)} \quad \forall \dot{X}_i(t) > \dot{X}_{i-1}(t) \quad (2.1)$$

with  $\dot{X}_i$  denoting the speed of vehicle  $i$ ,  $X_i$  the position of vehicle  $i$ ,  $l_i$  the length of vehicle  $i$  and  $i - 1$  the vehicle ahead of vehicle  $i$ . For vehicles (5 metres in length) travelling at 50 kph and approaching a stationary vehicle 24 metres ahead, the TTC would be equal to 1 second.

**Definition 4** *Offset in the context of this thesis is defined as the lateral distance from the centre of the ego vehicle to the centre of a surrounding vehicle (either leading or trailing) in the same lane.*

Figure 2.1 depicts the offset between an ego vehicle shown in red and a leading vehicle shown in green.

**Definition 5** *The time gap between a vehicle and a reference position in the context of this thesis is defined as the time required for the vehicle to reach the reference position.*

For example, in the scenario as shown in Figure 2.2, the time gap between the ego vehicle (depicted in red) and a leading vehicle (depicted in green) is defined as the time required for the ego vehicle to reach the position of the leading vehicle, i.e, to reach  $X_{Final}$  from  $X_{Initial}$  at velocity  $V_{Initial}$ .

**Definition 6** *In the context of this thesis, critical zone with respect to a vehicle is defined as the zone around the surrounding vehicles which should not be entered by the vehicle in order to guarantee that a collision can be avoided by executing an evasive action in an emergency.*

For example, in the traffic scenario as shown in Figure 2.3, the shaded area depicted by tan colour around the surrounding vehicles is an illustration of the critical zone to be maintained. This critical zone represented in this figure is calculated using time gap as the safety indicator, where a minimum distance has to be maintained between vehicles depending on the velocity and the capability of the ego vehicle to

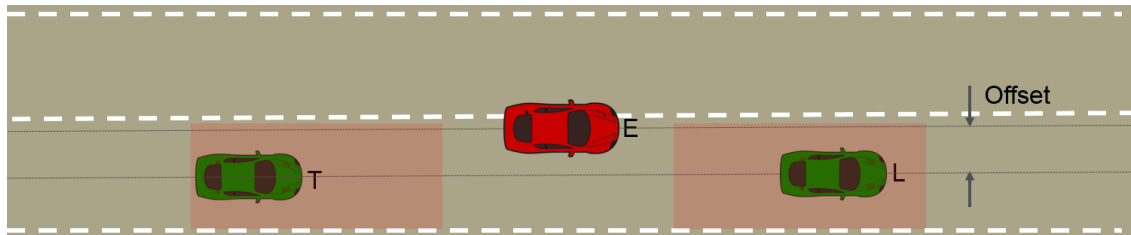


**Figure 2.1:** Lateral offset between the two vehicles. The ego vehicle is shown in red and the leading vehicle is shown in green.

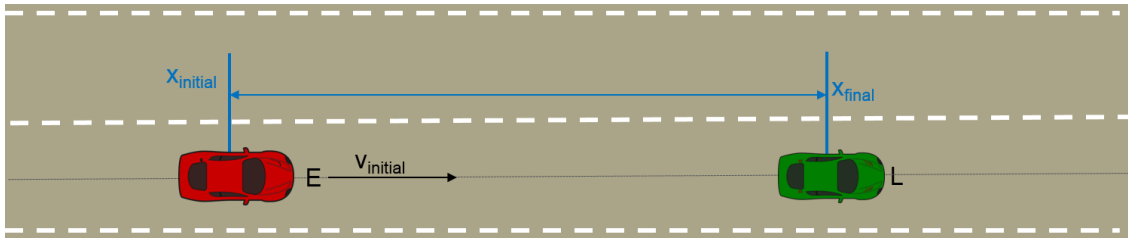


**Figure 2.2:** Time gap between two vehicles. The ego vehicle depicted in red has  $X_{Initial}$  as the longitudinal position with velocity  $V_{Initial}$ . The leading vehicle depicted in green in front of it has the position  $X_{Final}$ .

brake in order to avoid a collision. However, the ego vehicle can also steer away to avoid a collision and the critical zone to be maintained based on the braking or steering capability of the ego vehicle is explored in this thesis.

## 2.2 Problem description

A lane change manoeuvre is defined as complete when the ego vehicle positions itself in an adjacent lane safely, without any collision during the entire manoeuvre. For example, consider the traffic scenario depicted in Figure 2.3. The ego vehicle, shown in red drives in an initial host lane while being preceded by a leading vehicle L1 and followed by a trailing vehicle T1. The adjacent lane consists of two vehicles, a leading vehicle L2 and a trailing vehicle T2. The shaded area depicted by red colour around the surrounding vehicles is a critical zone which the ego vehicle should not enter in order to remain safe at all times. As described in the previous section, this critical zone represented is calculated by using a constant time gap as the safety indicator. The edges of the critical zone are given by the constant time gap to be maintained to initiate an evasive action. In addition, the critical zone around the surrounding vehicles is modelled on an assumed worst case behaviour. For example, in the case of a leading vehicle it is assumed that the leading vehicle comes to an immediate stop at any instant. The reason for this assumption could be attributed to the limitations in the sensing capability where ego vehicle does not have more information about the environment ahead of the leading vehicle. This assumption also gives the opportunity for the ego vehicle to initiate braking and avoid collision in case of unexpected emergencies like the leading vehicle actually crashing to a stop. Therefore a safe lane change by the ego vehicle can be guaranteed by ensuring the ego vehicle does not enter the critical zone during the entire lane change manoeuvre.

One of the commonly used manoeuvres in order to avoid an unforeseen lane change crash is to abort the lane change and return back to the host lane [25]. Such lane change abortion can be due to various reasons. For example, behaviour of the surrounding vehicles deviating from normal traffic behaviour can lead to such cases. The leading vehicle coming to an immediate stop due to a crash or the trailing vehicle accelerating (emergency vehicles, aggressive drivers) can be a few examples. In such cases, the ego vehicle is required to complete the lane change abortion by

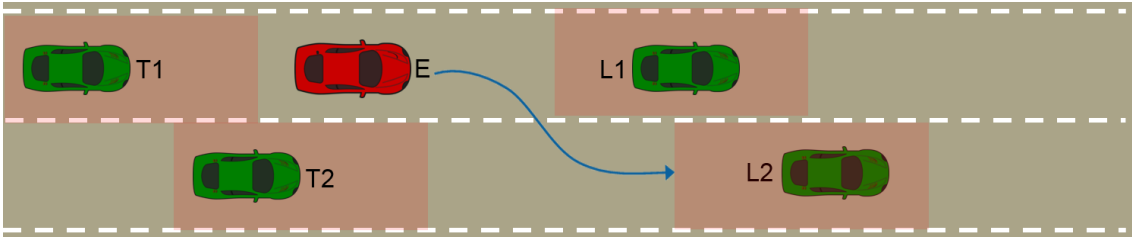


**Figure 2.3:** Traffic scenario with vehicles travelling in two lanes. Ego vehicle is shown in red. T1 and T2 are trailing vehicles. L1 and L2 are leading vehicles. Shaded area depicted by red colour is the critical zone.

following a path without any collision and the motion planning for the lane change manoeuvre should be able to handle such emergencies.

The position of the ego vehicle in the lane change manoeuvre and the lane change abort manoeuvre is determined based on the motion of the surrounding vehicles. However, it can be seen that the different scenarios during any lane change/lane abort manoeuvres can be formulated to be different versions of the same problem, i.e., motion planning for the ego vehicle to safely position itself between two surrounding vehicles in a target lane.

The problem of motion planning during lane change manoeuvres for autonomous vehicles with abort ability can therefore be simplified and formulated as follows: determine a feasible path for the longitudinal and lateral motion of the ego vehicle to position itself in a target lane with the ability to abort without any collision during the entire manoeuvre. *A collision free motion with the ability to abort during the longitudinal and lateral motion is guaranteed by determining the critical zone around the surrounding vehicles and ensuring that the ego vehicle remains outside the zones.* As long as the ego vehicle does not enter the critical zone, an evasive motion is possible satisfying the safety requirements. The motion planning algorithm proposed in this thesis can be summarised in the following steps:

1. Determine the critical zone around the surrounding vehicles in order to ensure a safe and feasible manoeuvre by the ego vehicle.
2. Find the desired final position between two vehicles in the target lane where the ego vehicle can be positioned when the manoeuvre is completed.
3. Plan the longitudinal motion to reach the desired position safely.
4. For a given longitudinal trajectory, plan the lateral motion for the ego vehicle to complete the lane change with the possibility to initiate the evasive action for abortion.

### 2.3 Vehicle model

Safety is an important aspect in the development of Advanced Driver Assistance (ADAS) functions for autonomous vehicles and evaluation of the severity of critical

situations plays a vital role. In order to evaluate such safety critical scenarios, having a mathematical model which describes the motion of the ego vehicle over the near future becomes very important. Motion prediction models can be categorised based on the level of abstraction. A comparison of the different methods, with different levels of abstraction, are discussed in detail in [19]. This section describes the point mass vehicle model used in the implementation of the proposed algorithm.

### 2.3.1 Point mass vehicle model

In the point mass vehicle model, the vehicle is considered to be an object with a finite mass and the vehicle motion is described as a function of time only based on the kinematic relations between the parameters of interest like position, velocity and acceleration. A significant advantage in using this model to describe the motion is the simplicity of the model. A comparison of different kinematic motion models is available in [20]. One of the common kinematic model is the Constant Acceleration (CA) model which is characterised by the equations of motion as

$$v = v_0 + at \quad (2.2)$$

$$x = x_0 + v_0t + \frac{1}{2}at^2 \quad (2.3)$$

where  $a$  is the constant acceleration,  $x_0$  and  $v_0$  denote the initial position and initial velocity and  $x$  and  $v$  denote the final position and final velocity respectively. A third equation of motion which is also commonly used in calculations can be derived from the above equations and is given by

$$v^2 = v_0^2 + 2a(x - x_0). \quad (2.4)$$

Another approximation of the vehicle motion using kinematic relationships between the parameters is the constant jerk model. Jerk is the third derivative of displacement and the equations characterising the constant jerk model are

$$a = a_0 + jt \quad (2.5)$$

$$v = v_0 + a_0t + \frac{1}{2}jt^2 \quad (2.6)$$

$$x = x_0 + v_0t + \frac{1}{2}a_0t^2 + \frac{1}{6}jt^3 \quad (2.7)$$

where  $j$  is the constant jerk and  $a_0$  is the initial acceleration. The constant jerk model can be used to model vehicle motion where the acceleration is not constant and it should be noted that a zero jerk value in the constant jerk model results in the constant acceleration model.

It is to be noted that the point mass model can be used to describe the motion of the vehicle in any direction, i.e., longitudinal and lateral. A state space representation can be obtained by discretising (2.5) - (2.7). The state space model describing the longitudinal motion of the vehicle is given by

$$\begin{bmatrix} x(k+1) \\ v_x(k+1) \\ a_x(k+1) \end{bmatrix} = \begin{bmatrix} 1 & t_s & \frac{t_s^2}{2} \\ 0 & 1 & t_s \\ 0 & 0 & 1 \end{bmatrix} \begin{bmatrix} x(k) \\ v_x(k) \\ a_x(k) \end{bmatrix} + \begin{bmatrix} \frac{t_s^3}{6} \\ \frac{t_s^2}{2} \\ t_s \end{bmatrix} [j_x(k)] \quad (2.8)$$

and the model describing the lateral motion of the vehicle is given by

$$\begin{bmatrix} y(k+1) \\ v_y(k+1) \\ a_y(k+1) \end{bmatrix} = \begin{bmatrix} 1 & t_s & \frac{t_s^2}{2} \\ 0 & 1 & t_s \\ 0 & 0 & 1 \end{bmatrix} \begin{bmatrix} y(k) \\ v_y(k) \\ a_y(k) \end{bmatrix} + \begin{bmatrix} \frac{t_s^3}{6} \\ \frac{t_s^2}{2} \\ t_s \end{bmatrix} [j_y(k)] \quad (2.9)$$

where  $t_s$  is the sample time. Although a kinematic model for vehicle motion gives the advantage of simplicity, it does not account for the dynamics of the vehicle and therefore requires suitable approximations to be made while designing any control algorithm using this model. The point mass model is used to describe the vehicle motion in determining the critical zone and the motion planning which is described in the next chapter.

# 3

## Methods

This chapter deals with the methods used to solve the problem of motion planning during lane change as described in the previous chapters. The chapter also includes a description of their respective implementations. The chapter is structured into four sections where each section deals with each of the four major steps included in the proposed motion planning algorithm as discussed in the previous chapter. MATLAB is used as the programming language to implement the described methods and also for the illustration of the results.

### 3.1 Critical zone

Critical zone, as defined in the previous chapter, can be considered as a measure to guarantee the safety of the autonomous vehicle. For example, in the traffic scenario as shown in Figure 2.3, the critical zone depicted is calculated using time gap as the safety indicator. In this case a constant value of time gap is used as the measure to initiate the evasive action in case of emergencies. This value of time gap gives the minimum distance that has to be maintained between vehicles depending on the velocity of the ego vehicle and the capability of the ego vehicle to brake in order to avoid a collision. Being a very simplistic approach, this method of definition for the critical zones has the disadvantage that when a considerable offset is present between the vehicles, it would be possible to avoid a collision by using a steering action. In such cases, initiating a braking action might not be the desirable action for the user and might also not be the best manoeuvre in certain traffic scenarios. Ensuring the availability of a safe evasive manoeuvre by using the steering capability also gives the ego vehicle the opportunity to show intention to perform lane in dense traffic scenarios. Therefore, making use of the braking and the steering capability of the ego vehicle to avoid a collision can result in reducing the critical zone around the surrounding vehicles compared to the constant time gap method and this approach is explained in the following sections.

#### 3.1.1 Assumptions in critical zone modelling

In order to model the critical zone around the surrounding vehicles, it is required to have a few assumptions to model the motion of the surrounding vehicles and also the

severity of the evasive manoeuvre that the ego vehicle performs to avoid a collision. The assumptions used in the modelling of the critical zone are

- The surrounding vehicles are considered to have a constant velocity motion when the ego vehicle initiates and performs the lane change manoeuvre. This constant velocity motion is considered to be the nominal behaviour of the vehicles involved in the traffic scenario.
- The critical zone calculated around the surrounding vehicles at every instant is based on an assumed worst case behaviour. This assumed behaviour is considered to predict the critical zones and the desired final position for the ego vehicle at the end of the lane change manoeuvre. It should also be noted that this worst case scenario for the surrounding vehicles forces the ego vehicle to initiate the evasive manoeuvre when required.
- The ego vehicle's motion is modelled using a point mass model for both the longitudinal and the lateral motion during the lane change manoeuvre and the evasive manoeuvre.
- During the evasive manoeuvre the ego vehicle uses a pre-defined longitudinal and lateral acceleration profile. The assumed acceleration profiles are modelled based on the severity of the evasive action and are explained in detail in the next section.

#### 3.1.2 Acceleration profiles

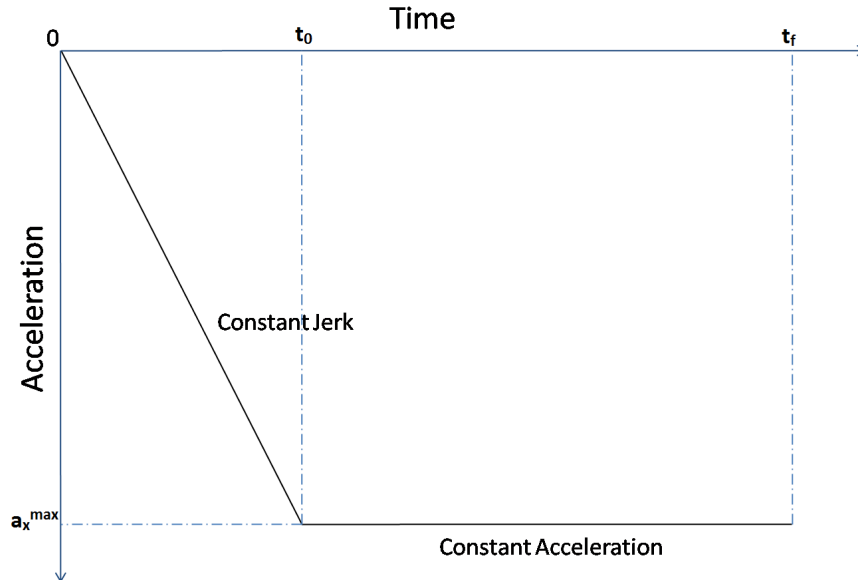


**Figure 3.1:** The longitudinal acceleration profile for braking. The ego vehicle is modelled to follow a constant jerk profile until time  $t_0$ , where it reaches the maximum deceleration limit,  $a_x^{\max}$ . The vehicle follows a constant acceleration profile from time  $t_0$  to final time  $t_f$ .

The longitudinal and lateral acceleration profiles of the ego vehicle during the evasive manoeuvre needs to be assumed based on the braking and steering capabilities of the ego vehicle. These acceleration profiles must accommodate the best manoeuvring capability of the ego vehicle to avoid collisions in case of emergency situations. It should also be noted that there is always the flexibility to assume different acceleration profiles in order to have a soft evasive manoeuvre or a more severe, hard evasive manoeuvre based on the acceleration limits.

For longitudinal acceleration profile, the braking behaviour is modelled based on the maximum deceleration and maximum jerk capabilities of the vehicle as shown in Figure 3.1.

For lateral acceleration profile, the steering behaviour is modelled based on the limits for jerk, acceleration and velocity on the lateral manoeuvring capability of the vehicle. The lateral acceleration is modelled as shown in Figure 3.2.

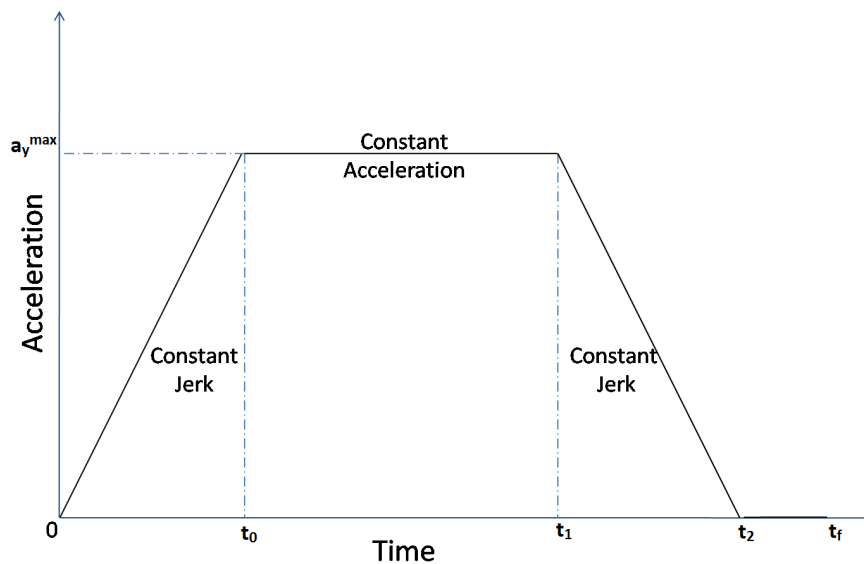


**Figure 3.2:** The lateral acceleration profile for steering. The ego vehicle is modelled to follow a constant jerk profile until time  $t_0$ , where it reaches the maximum acceleration  $a_y^{max}$ . The ego vehicle follows a constant acceleration profile from time  $t_0$  to  $t_1$ . From  $t_1$  to  $t_2$ , it follows a deceleration profile with constant jerk until zero acceleration is achieved. Constant zero acceleration is maintained from time  $t_2$  to final time  $t_f$ .

### 3.1.2.1 Determining lateral acceleration profile for a fixed lane width

While predetermining the lateral acceleration profile for steering evasive manoeuvre, the lane limitations also needs to be considered. The evasive manoeuvre should ensure that the ego vehicle does not steer out of the host lane after avoiding the collision with the vehicle in the adjacent target lane. Figure 3.3 shows the complete steering evasive manoeuvre profile. Between time 0 to  $t_3$ , the ego vehicle can travel the minimum lateral safety distance in order to successfully steer away from a col-

lision. Once this is accomplished, it has to be noted that the ego vehicle will have picked up some lateral velocity. Subsequently, ego vehicle must be able to reduce its lateral velocity to zero within the limits of the host lane between time  $t_3$  and  $t_6$ . This would ensure that the ego vehicle does not overshoot the host lane limits after initiating the evasive manoeuvre from the target lane. The acceleration profile between time 0 to  $t_2$  is anti-symmetric to acceleration profile between time  $t_3$  and  $t_6$ . The ego vehicle reaches the max lateral velocity at time  $t_2$  and maintains it till time  $t_3$ .

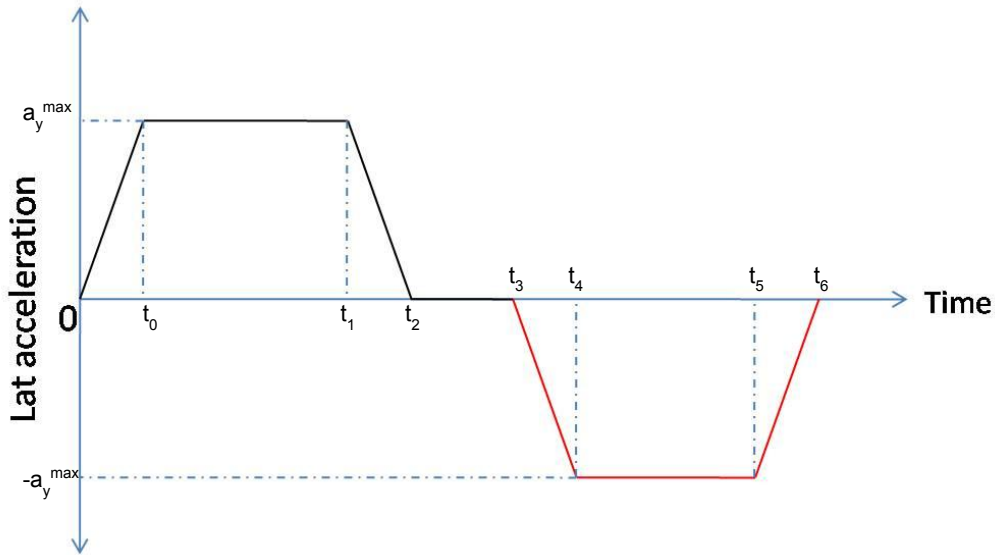


**Figure 3.3:** Complete acceleration profile for steering evasive manoeuvre. The black curve indicates the evasive steering from the target lane for the ego vehicle to avoid collision and the red curve indicates the ego vehicle’s manoeuvre back into the host lane.

The time parameters  $t_3$ ,  $t_4$ ,  $t_5$  and  $t_6$  are dependant on the maximum lateral velocity and the lane width. The lateral velocity for the ego vehicle is the maximum lateral velocity at time  $t_3$  and should be 0 m/s at time  $t_6$ . Also, the distance travelled between time  $t_3$  to time  $t_6$  should be less than the lane width. It has to be noted that time elapsed between time  $t_3$  and time  $t_4$  is the same as time elapsed between time  $t_5$  to time  $t_6$ . Using these dependencies, the time parameters  $t_0$ ,  $t_1$  and  $t_2$  can

be calculated using the following set of equations.

$$S_{(t_3-t_4)} = v_y^{max}(t_4 - t_3) - \frac{j_y^{max}(t_4 - t_3)^3}{6} \quad (3.1)$$

$$V_{t_4} = v_y^{max} - \frac{j_y^{max}(t_4 - t_3)^2}{2} \quad (3.2)$$

$$S_{(t_4-t_5)} = S_{(t_3-t_4)} + V_{t_4}(t_5 - t_4) - \frac{a_y^{max}(t_5 - t_4)^2}{2} \quad (3.3)$$

$$V_{t_5} = v_{t_4} - a_y^{max}(t_5 - t_4) \quad (3.4)$$

$$W_{lane} = S_{(t_4-t_5)} + V_{t_5}(t_6 - t_5) - \frac{a_y^{max}(t_6 - t_5)^2}{2} + \frac{j_y^{max}(t_6 - t_5)^3}{6} \quad (3.5)$$

$$0 = V_{t_5} - a_y^{max}(t_6 - t_5) + \frac{j_y^{max}(t_6 - t_5)^2}{2} \quad (3.6)$$

$$t_0 = t_4 - t_3 = t_6 - t_5 = t_2 - t_1 \quad (3.7)$$

$$t_1 - t_0 = t_5 - t_4 \quad (3.8)$$

where  $a_y^{max}$ ,  $j_y^{max}$  and  $v_y^{max}$  denote the maximum lateral acceleration, maximum lateral jerk and maximum lateral velocity respectively.  $W_{lane}$  denotes the width of the lane.  $S_{(t_3-t_4)}$ ,  $V_{t_4}$  represent the lateral displacement and velocity at time  $t_4$  respectively.  $S_{(t_4-t_5)}$ ,  $V_{t_5}$  represent the lateral displacement and velocity at time  $t_5$ .

### 3.1.3 Leading vehicles in adjacent lane

In order to model the critical zone around the leading vehicle, a critical time defined as the latest time before which the ego vehicle has to initiate an emergency action to avoid collision is calculated based on specific assumptions. The leading vehicle is assumed to travel with a constant velocity motion and come to an immediate stop anytime as depicted in Figure 3.4. Therefore, in this case, the critical zone around the leading vehicle is defined as the minimum distance to be maintained between the ego vehicle and the leading vehicle so that a collision avoidance can be guaranteed by executing the evasive manoeuvre. During emergency manoeuvres, i.e., braking or steering to avoid a collision, the ego vehicle is assumed to follow the respective acceleration profiles described in Section 3.1.2.

For a vehicle travelling at a given velocity, the braking distance can be defined as the distance the vehicle travels before slowing down to a complete stop. In other words, it is the distance travelled by the vehicle to reach a final longitudinal velocity of zero and this distance can be calculated from (2.4) using the values from assumed acceleration profile. The critical time to be maintained by the ego vehicle to avoid collision with the leading vehicle by initiating braking is then calculated using the braking distance of the ego vehicle,  $S_{ego}$  at a velocity  $v_{ego}$  as

$$T_{brake} = \frac{S_{ego} + S_{min}}{v_{ego}} \quad (3.9)$$

where  $T_{brake}$  denotes the critical time gap for initiating braking and  $S_{min}$  is the minimum longitudinal safety gap between the two vehicles after stopping.

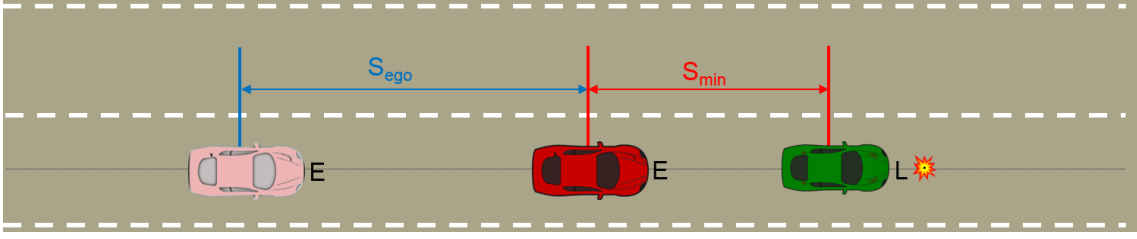


**Figure 3.4:** Critical zone calculation for the leading vehicle when the ego vehicle brakes to avoid a collision. Ego vehicle denoted by E is represented in red colour and the leading vehicle denoted by L is depicted in green colour.

The ego vehicle can also steer away to avoid collision with the leading vehicle in certain traffic situations depending on the offset. In such cases, the critical time to be maintained is calculated as the time required for the ego vehicle to travel a safe distance laterally, thereby avoiding collision with the leading vehicle. For example, in Figure 3.5, if  $W_l$  and  $W_e$  denote the width of the leading vehicle and the width of the ego vehicle respectively,  $W_s$  is the minimum lateral safety gap between the two vehicles. The lateral safe distance,  $S_{\text{latsafe}}$  to be travelled by the ego vehicle can be calculated using

$$S_{\text{latsafe}} = 0.5W_l + 0.5W_e + W_s - \text{offset}. \quad (3.10)$$

The critical time to be maintained by the ego vehicle to avoid collision with the leading vehicle by initiating steering  $T_{\text{steer}}$  is then calculated as the time taken by the ego vehicle to travel the safe distance  $S_{\text{latsafe}}$  laterally with the assumed lateral acceleration profile (Figure 3.2).

$$v_0 = \frac{j_y^{\text{max}} t_0^2}{2} \quad (3.11)$$

$$s_0 = \frac{j_y^{\text{max}} t_0^3}{6} \quad (3.12)$$

$$v_1 = v_0 + a_y^{\text{max}}(t_1 - t_0) \quad (3.13)$$

$$s_1 = s_0 + v_0(t_1 - t_0) + \frac{a_y^{\text{max}}(t_1 - t_0)^2}{2} \quad (3.14)$$

$$s_2 = s_1 + v_1(t_2 - t_1) + \frac{a_y^{\text{max}}(t_2 - t_1)^2}{2} - \frac{j_y^{\text{max}}(t_2 - t_1)^3}{6} \quad (3.15)$$

$$s_3 = s_2 + v_y^{\text{max}}(t_f - t_2) \quad (3.16)$$

The value of  $t_0$ ,  $t_1$ ,  $t_2$  and  $t_f$  is calculated from (3.1)-(3.8). Comparing the value of  $S_{\text{latsafe}}$  with  $s_0$ ,  $s_1$ ,  $s_2$  and  $s_3$  we use the appropriate equation from (3.12), (3.14), (3.15) or (3.16) to solve for  $T_{\text{steer}}$ .

For example if the value of  $S_{\text{latsafe}}$  is between  $s_1$  and  $s_2$ , then equation 3.15 is used to solve for  $T_{\text{steer}}$

$$S_{\text{latsafe}} = s_1 + v_1 t_{\text{str}} + \frac{a_y^{\text{max}} t_{\text{str}}^2}{2} - \frac{j_y^{\text{max}} t_{\text{str}}^3}{6} \quad (3.17)$$

$$T_{\text{steer}} = t_{\text{str}} + t_1. \quad (3.18)$$

The critical time  $T_{\text{critical}}$  defined as the latest time before which the ego vehicle has to initiate an emergency action, i.e., either brake or steer to avoid the collision with the leading vehicle is given by:

$$T_{\text{critical}} = \min(T_{\text{brake}}, T_{\text{steer}}). \quad (3.19)$$

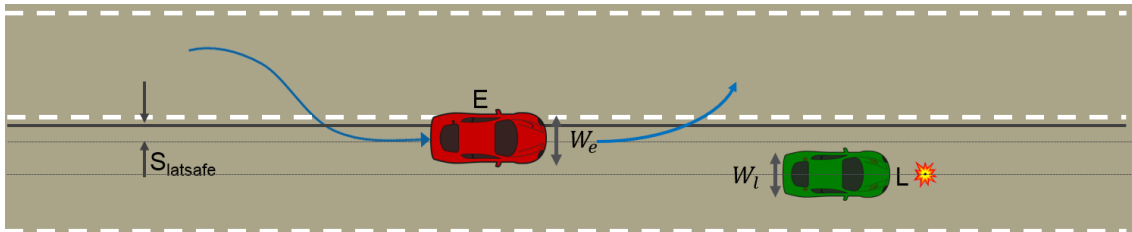


**Figure 3.5:** Critical zone calculation for the leading vehicle when the ego vehicle steers to avoid a collision. Ego vehicle denoted by E is represented in red colour and the leading vehicle denoted by L is depicted in green colour.

This critical time  $T_{\text{critical}}$  is calculated for every possible offset value of the ego vehicle. Finally, the critical zone around the leading vehicle is then obtained by using  $T_{\text{critical}}$  and the velocity  $v_{\text{ego}}$ . By ensuring that the ego vehicle is not positioned in the critical zone at any time, the collision avoidance is guaranteed by allowing enough time for the ego vehicle to initiate an emergency manoeuvre. The assumptions hold true for leading vehicles in any target lane and therefore the critical zone calculated using this method can be used for path planning during the lane change or path planning during the lane change abort manoeuvre.

### 3.1.4 Trailing vehicles in adjacent lane

Similar to the case of leading vehicle, the ego vehicle and the trailing vehicle should maintain a minimum distance between them to ensure safe driving conditions. However only the motion of the ego vehicle can be controlled and not of the trailing vehicle. It is the responsibility of the trailing vehicle to maintain a safe distance behind the ego vehicle. Therefore, the critical zone around the trailing vehicle is modelled by calculating a critical time before which the ego vehicle has to initiate an emergency action to avoid collision.

The assumptions for the motion of the trailing vehicle is different from that of the leading vehicle. When the ego vehicle is executing a lane change, all the possible behaviours of the trailing vehicle approaching from behind needs to be accounted for. As such it may respond in three different ways, it can decelerate to let the ego vehicle complete the lane change. It can fail to notice the ego vehicle and continue in its current state or it can accelerate in order to cut off the ego vehicle from lane changing.

The worst case scenario will be when the approaching vehicle accelerates in order to cut off the ego vehicle's manoeuvre. A constant acceleration model is assumed for the trailing vehicle. The time taken by the ego vehicle to abandon the lane change

and move away from the path of the approaching vehicle is taken as the critical time as illustrated in Figure 3.6.

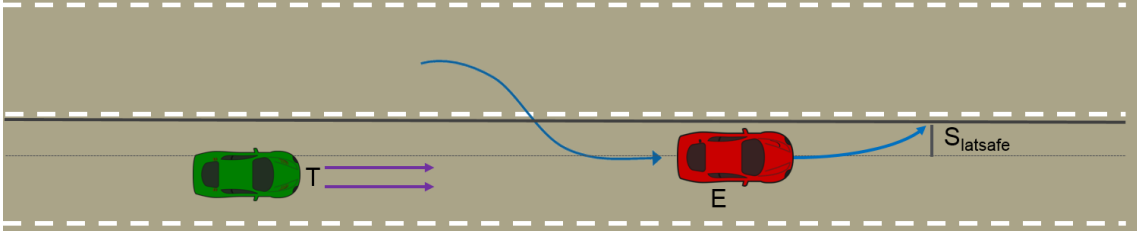


**Figure 3.6:** Critical time calculation for trailing vehicle in adjacent lane.  $S_{latsafe}$  is the minimum distance required to travel for the ego vehicle E to avoid a collision with the trailing vehicle T. The dotted line represent the safe width limit and the thick line denote the lane limits.

$T_{critical}$  is the time at which the ego vehicle travels the minimum distance to safely get away from the path of the approaching vehicle, laterally. The lateral minimum safe distance,  $S_{latsafe}$  to be travelled by the ego vehicle is calculated as shown in equation 3.10.

$$T_{critical} = T_{S_{egoLateral}=S_{latsafe}} \quad (3.20)$$

$T_{critical}$  is calculated for all possible offsets in front of the trailing vehicle, from (3.11)-(3.16). However, when critical zone around the trailing vehicle needs to be calculated a constant acceleration model is assumed for the oncoming trailing vehicle. The safety critical distance for a given offset is determined as

$$S_{ego} = v_{ego}T_{critical} \quad (3.21)$$

$$S_{trail} = v_{trail}T_{critical} + \frac{a_{trail}T_{critical}^2}{2} \quad (3.22)$$

$$S_{critical} = \max((S_{trail} - S_{ego}), S_{min}) \quad (3.23)$$

where  $v_{ego}$  and  $v_{trail}$  are the longitudinal velocities of ego vehicle and trailing vehicle respectively.  $a_{trail}$  is the assumed constant acceleration for the trailing vehicle.  $S_{min}$  is the minimum critical distance to be maintained in front of trailing vehicle.  $S_{critical}$  calculated for every offset around the trailing vehicle to formulate its critical zone.

#### 3.1.5 Vehicles in host lane

For vehicles in the host lane, the critical zone is calculated based on different assumptions compared to the critical zone for vehicles in the adjacent lane. Although the method used for calculating the critical zone for vehicles in the adjacent lane can be extended to vehicles in the host lane, avoiding collision by steering away from vehicles in the host lane during lane change or lane change abort manoeuvre is not a very common traffic behaviour. Therefore the capability of the ego vehicle to steer away from vehicles in the host lane can be ignored. By considering only

braking as the emergency action by the ego vehicle to avoid a collision, the problem can be made simpler and still be valid in a wider range of traffic scenarios.

In case of the leading vehicle in the host lane, the worst case assumption is that the leading vehicle brakes hard to a stop. However, since braking is the only emergency action performed by the ego vehicle, the critical time  $T_{\text{critical}}$  is equal to the time to be maintained by the ego vehicle to initiate braking. This time,  $T_{\text{brakeLead}}$  is calculated in a way similar to  $T_{\text{brake}}$  in (3.9).  $T_{\text{brakeLead}}$  calculated based on the braking distance and relative velocity between the two vehicles as

$$T_{\text{brakeLead}} = \frac{S_{\text{ego}} - S_{\text{leading}} + S_{\text{min}}}{v_{\text{ego}}} \quad (3.24)$$

where  $S_{\text{ego}}$  and  $S_{\text{leading}}$  are the braking distances of the ego vehicle and the leading vehicle respectively and  $S_{\text{min}}$  is the minimum safety distance to be maintained.

It should be noted that  $T_{\text{brakeLead}}$  calculated in (3.24) is different from  $T_{\text{brake}}$  in (3.9) because the leading vehicle in the host lane is considered to brake to a stop as opposed to the case in the target lane where the leading vehicle is considered to come to an immediate stop at any time. This assumption is relaxed owing to the fact that the probability of both the leading vehicles coming to an immediate stop in an actual traffic scenario is very minimal.

In case of the trailing vehicle, it is assumed that the trailing vehicle will not accelerate in order to intentionally cause a collision with the ego vehicle. Therefore trailing vehicle in the host lane is considered to have a constant velocity model with a constant lateral position. The trailing vehicle however, is also able to brake hard in case of emergencies with a defined deceleration profile, given enough reaction time. The worst case in this scenario will be when the ego vehicle brakes hard to a stop. The critical time  $T_{\text{critical}}$  is equal to the time to be maintained by the ego vehicle to initiate braking. This time denoted as  $T_{\text{brakeTrail}}$  is also calculated based on the braking distances and the relative velocity between the two vehicles.  $T_{\text{brakeTrail}}$  is given by

$$T_{\text{brakeTrail}} = \frac{S_{\text{trailing}} - S_{\text{ego}} + S_{\text{min}}}{v_{\text{trailing}}} + t_{\text{reaction}} \quad (3.25)$$

where  $S_{\text{ego}}$  and  $S_{\text{trailing}}$  are the braking distances of the ego vehicle and the trailing vehicle respectively and  $S_{\text{min}}$  is the minimum safety distance to be maintained.

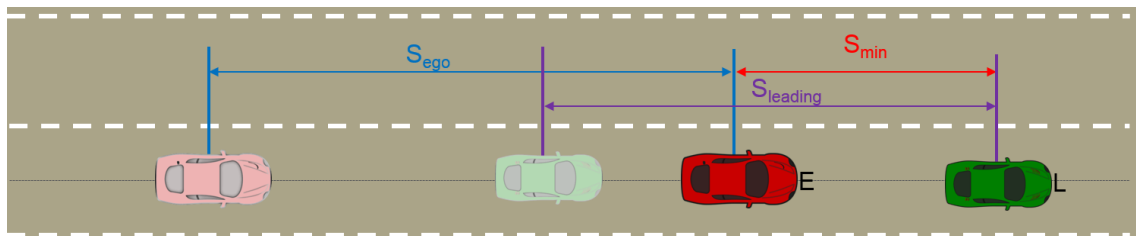


**Figure 3.7:** Critical time calculation for leading vehicle in host lane.  $S_{\text{leading}}$  and  $S_{\text{ego}}$  being the braking distance travelled by the leading vehicle L and ego vehicle E respectively. The dotted line represents the lane centres and the thick line denotes the lane limits.

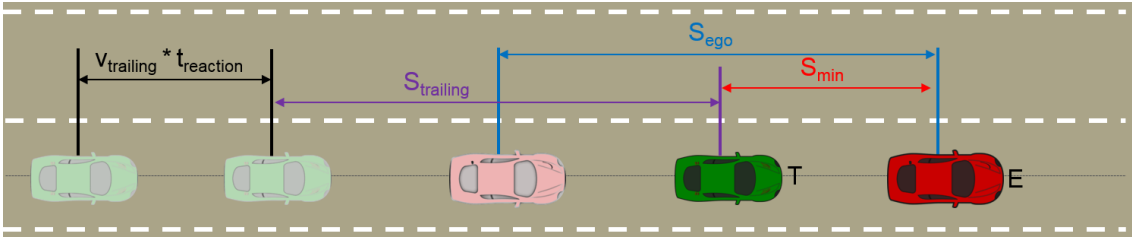


**Figure 3.8:** Critical time calculation for trailing vehicle in host lane.  $S_{trailing}$  and  $S_{ego}$  being the braking distance travelled by the trailing vehicle T and ego vehicle E respectively. The dotted line represents the lane centres and the thick line denotes the lane limits.

$t_{reaction}$  denotes the reaction time for the trailing vehicle to initiate braking. An illustration of the distances used in the calculation of the critical zone for this case can be seen in Figure 3.8. The braking distances for the vehicles are calculated based on assumed deceleration profiles similar to Figure 3.1.

*Remark:* Although the methods for modelling the critical zone for vehicles in the host lane are discussed here, the simulation results presented in Chapter 4 do not include vehicles or other objects in the host lane.

## 3.2 Desired final position

During normal driving conditions, it is desirable that the ego vehicle positions itself in the centre of the lane. Therefore for any lane change manoeuvre planning, it is important that the ego vehicle positions itself in the centre of the target lane or as close as possible to the centre of the target lane without risking safety. This would mean that the ego vehicle should be able to squeeze into gaps between the leading and trailing vehicles in the target lane without violating the critical zone around those vehicles. For example in the traffic situation depicted in Figure 3.9, the ego vehicle can plan a manoeuvre to position itself in the centre of the lane without entering the critical zone.

However, for a scenario as shown in Figure 3.10, where the critical zones of the leading vehicle and the trailing vehicle overlap each other, the ego vehicle cannot position itself in the centre of the target lane. In such cases, the intersection of the critical zones around the leading and the trailing vehicles will be the desired final position to plan the ego vehicle's motion. Since the critical zones around the surrounding vehicles are calculated with respect to the centre of the ego vehicle, positioning the centre of the ego vehicle at the intersection of the critical zones would mean that the ego vehicle is positioned as close as possible to the centre of the target lane and still have enough time to initiate an evasive manoeuvre in case of emergencies.

In order to find the intersection between the two critical zones, analytical expressions for the critical zones around the predicted final positions of the surrounding vehicles

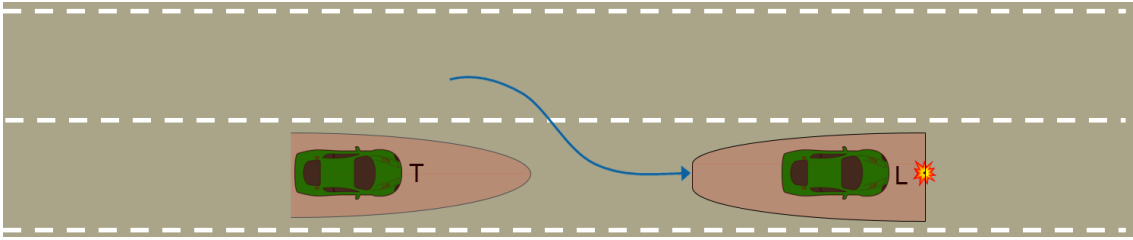


**Figure 3.9:** Scenario where the ego vehicle can manoeuvre into the centre of the target lane. The predicted final positions of the leading and trailing vehicle at the end of lane change time, with their critical zones are shown. The blue line represents the trajectory of the ego vehicle, during the lane change.

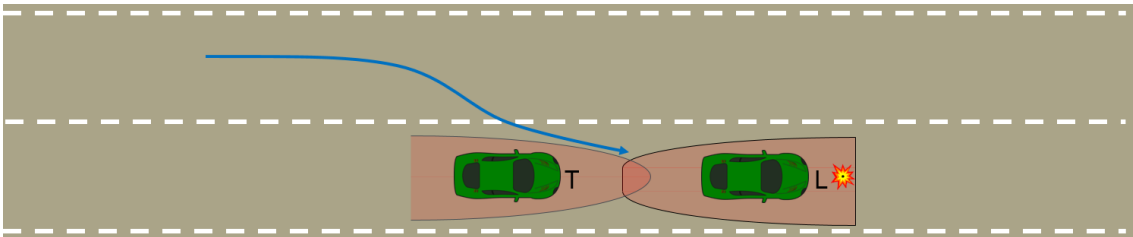


**Figure 3.10:** Scenario where ego vehicle positions itself at the intersection of the critical zones of surrounding vehicle at the end of the lane change time. The predicted final positions of the leading and trailing vehicle at the end of lane change time, with their critical zones are shown. The blue line represents the trajectory of the ego vehicle, during the lane change.

are derived. The lateral and the longitudinal positions of the critical zone limits around a vehicle can be independently expressed as functions of critical time,  $T_{\text{critical}}$ . The intersection between the two zones can then be calculated by solving these set of expressions. The steps used to find the desired final position is summarised in Table 3.1.

### 3.3 Longitudinal motion planning

The final steps in the proposed algorithm includes the motion planning in the longitudinal and the lateral direction to reach the desired final position without entering the critical zones around the surrounding vehicles. In addition to constraints on position of the ego vehicle during the motion planning, care should also be taken in making sure the ego vehicle does not plan a motion which cannot be executed during the evasive manoeuvre due to physical limitations like actuator saturation and lane widths. Owing to the presence of such constraints, one of the natural choices for motion planning is the use of Model Predictive Control (MPC) using the receding horizon idea.

In MPC, the control design includes constraints as an intrinsic part of the system. At any given sampling time, the current knowledge of the system is used to predict the response over a finite future by the controller. This also gives the controller the

**Table 3.1:** Steps to calculate the intersection point of the critical zones around the predicted final positions of the leading and trailing vehicles.

<b>Finding intersection</b>	
1:	Determine the expression for the longitudinal positions of critical zone limits, $X_{\text{critical}}(T_{\text{critical}})$ as a function of $T_{\text{critical}}$ . ( $X_{\text{Trail}}(T_{\text{critical}})$ for the trailing vehicle and, $X_{\text{LeadBrake}}(T_{\text{critical}})$ and $X_{\text{LeadSteer}}(T_{\text{critical}})$ ) for the leading vehicle.
2:	Determine the expression for the lateral positions of critical zone limits, $Y_{\text{critical}}(T_{\text{critical}})$ as a function of $T_{\text{critical}}$ . ( $Y_{\text{Trail}}(T_{\text{critical}})$ for the trailing vehicle and, $Y_{\text{LeadBrake}}(T_{\text{critical}})$ and $Y_{\text{LeadSteer}}(T_{\text{critical}})$ ) for the leading vehicle.
3:	Solve $X_{\text{LeadBrake}}(T_{\text{critical}}) == X_{\text{Trail}}(T_{\text{critical}})$ and $X_{\text{LeadSteer}}(T_{\text{critical}}) == X_{\text{Trail}}(T_{\text{critical}})$ . Choose the valid real solution as $T_{\text{intersect}}$ .
4:	Substitute the value of $T_{\text{intersect}}$ in the longitudinal expressions from Step 1 to find the value of $X_{\text{intersect}}$ and in the lateral expressions from Step 2 to find the value of $Y_{\text{intersect}}$ .
5:	If a valid real solution cannot be determined for $T_{\text{intersect}}$ in Step 3, the lateral position of the leading vehicle is taken as $Y_{\text{intersect}}$ .
6:	Substitute the value of $Y_{\text{intersect}}$ from Step 5 in the lateral expressions for $Y_{\text{LeadSteer}}(T_{\text{critical}})$ and $Y_{\text{LeadBrake}}(T_{\text{critical}})$ from Step 2 to find the value of $T_{\text{intersect}}$ .
7:	Substitute the value of $T_{\text{intersect}}$ from Step 6 in the lateral expressions from Step 1 to find the value of $X_{\text{intersect}}$ .

chance to predict if the system can reach any of the constraints. More information about predictive control with constraints can be found in [31]. According to [30], the receding horizon idea used in MPC can be summarised in three steps:

- At time instant  $k$ , predict response over a finite prediction horizon depending on the sequence of future control inputs.
- Pick the control input sequence which gives the best performance in terms of a cost function and respecting the constraints
- Apply the first element of the control input sequence and discard the rest. Return to step 1.

The longitudinal motion planning is thus formulated as a Quadratic Programming (QP) optimisation problem. Model Predictive Control is used to solve the QP problem in terms of control commands. The vehicle motion is modelled using the discrete point mass model as described in section 2.3.1. Longitudinal position  $x$ , longitudinal velocity  $v_x$  and longitudinal acceleration  $a_x$  represent the states of the ego vehicle and the input to the system is the longitudinal jerk,  $j_x$ . The states and

the input are subjected to the following set of constraints:

$$x(k) \geq x_{min}(k) \quad (3.26)$$

$$x(k) \leq x_{max}(k) \quad (3.27)$$

$$v_{xmin} \leq v_x(k) \leq v_{xmax} \quad (3.28)$$

$$a_{xmin} \leq a_x(k) \leq a_{xmax} \quad (3.29)$$

$$j_{xmin} \leq j_x(k) \leq j_{xmax} \quad (3.30)$$

The constraints on longitudinal position  $x(k)$  denoted by (3.26) and (3.27) ensure that the planned manoeuvre stays within the longitudinal position limits. The inequalities denoted by equations (3.28) - (3.30) limit the longitudinal velocity, acceleration and jerk respectively and can be changed to either account for the actuator limitations or to account for a smooth manoeuvre.

In order to ensure that the vehicle's longitudinal position is driven to the desired final position, the state equations describing the longitudinal position are modified to include the deviation from the final desired position. The desired final position for the motion planning is given by  $X_{Intersect}$  as explained in Section 3.2. Given a desired final position  $x_{des}$ , the state equation for the longitudinal position from (2.9) can be rewritten in terms of deviation variable,  $\delta_x$  as:

$$x_{des} - x(k+1) = x_{des} - x(k) - t_s v_x(k) - \frac{t_s^2}{2} a_x(k) - \frac{t_s^3}{6} j_x(k) \quad (3.31)$$

$$\delta_x(k+1) = \delta_x(k) - t_s v_x(k) - \frac{t_s^2}{2} a_x(k) - \frac{t_s^3}{6} j_x(k) \quad (3.32)$$

Similarly, the limits on the longitudinal position can now be expressed in terms of the deviation variable as:

$$\delta_x(k) \geq \delta_{xmin}(k) \quad (3.33)$$

$$\delta_x(k) \leq \delta_{xmax}(k) \quad (3.34)$$

where  $\delta_{xmax}(k) = x_{des} - x_{min}(k)$  and  $\delta_{xmin}(k) = x_{des} - x_{max}(k)$  respectively.

The longitudinal motion planning to complete the lane change from an initial point to a desired final point, following the vehicle model and maintaining the constraints can now be written in the form of a standard QP optimisation problem as:

$$\min_z J = \frac{1}{2} z^T H z \quad (3.35)$$

$$s.t. A_{eq} z = B_{eq} \quad (3.36)$$

$$A_{in} z \leq B_{in} \quad (3.37)$$

where  $z = [\delta_x(k), v_x(k), a_x(k), j_x(k)]^T$  and the cost function to be minimised for the control problem is given by:

$$J = \sum_{i=0}^{N-1} (X(i)^T Q X(i) + u(i)^T R u(i)) + X(N)^T P_f X(N) \quad (3.38)$$

where  $X = [\delta_x(k), v_x(k), a_x(k)]^T$  are the states with weight  $Q$  as the stage cost and  $P_f$  as the terminal cost for the final state.  $u = [j_x(k)]$  is the control input to the system with weight  $R$  as the cost. By penalising the deviation from the final desired state ( $\delta_x(N) = 0, v_x(N) = 0, a_x(N) = 0$ ) using high weight values in  $P_f$ , the desired trajectory is derived.

### 3.4 Lateral motion planning

Having determined the safety constraints and a desired final position, for a given longitudinal trajectory, the lateral motion planning is formulated as a Quadratic Programming (QP) optimisation problem similar to the longitudinal motion planning. Model Predictive Control is used to solve the QP problem in terms of control commands. Since the point mass model can be used to model the longitudinal motion as well as the lateral motion, the vehicle motion used in the lateral motion planning is also modelled using the discrete point mass model as described in section 2.3.1. Lateral position  $y$ , lateral velocity  $v_y$  and lateral acceleration  $a_y$  represent the states of the ego vehicle and the input to the system is the lateral jerk,  $j_y$ . The states and the input are subjected to the following set of constraints:

$$y(k) \geq y_{min}(k) \tag{3.39}$$

$$y(k) \leq y_{max}(k) \tag{3.40}$$

$$v_{ymin} \leq v_y(k) \leq v_{ymax} \tag{3.41}$$

$$a_{ymin} \leq a_y(k) \leq a_{ymax} \tag{3.42}$$

$$j_{ymin} \leq j_y(k) \leq j_{ymax} \tag{3.43}$$

Similar to the constraints on the longitudinal motion, the lateral motion is also subjected to a set of constraints. The inequalities denoted by equations (3.41) - (3.43) limit the lateral velocity, acceleration and jerk respectively and can be changed to either account for the actuator limitations or to account for a smooth manoeuvre. The constraints on lateral position  $y(k)$  denoted by (3.39) and (3.40) ensure that the planned manoeuvre remains safe by not positioning the vehicle inside the critical zones.

The constraints on the lateral position varies with time and it is non-linear. This results in an MPC problem which is complicated to solve. However, the critical zone constraints are a function of  $T_{critical}$  and they can be pre-calculated over the entire horizon to turn the MPC problem, where the solution can be obtained in a relatively easier way. The steps to calculate the lateral position constraints are summarised in Table 3.2.

In order to ensure that the vehicle's lateral position is driven to the desired final position, the state equations describing the lateral position are modified to include the deviation from the final desired position. The desired final position for the motion planning is given by  $Y_{Intersect}$  as explained in Section 3.2. Given a desired final position  $y_{des}$ , the state equation for the lateral position from (2.9) can be

**Table 3.2:** Steps to determine the lateral constraints over the prediction horizon

<b>Finding the lateral constraints over the prediction horizon</b>	
1:	The longitudinal position $x(t)$ over the entire prediction horizon and the longitudinal positions of the critical zone limits $X_{\text{critical}}(T_{\text{critical}})$ are available as explained in Section 3.3 and Table 3.1 respectively. These relations can be used to find $T_{\text{critical}}$ for a given $x(t)$ .
2:	Substitute the value of $T_{\text{critical}}$ from Step 1 in the lateral expressions for the critical zone limits, $Y_{\text{critical}}(T_{\text{critical}})$ to find the lateral constraints over the prediction horizon.
3:	If a real and a valid value for $T_{\text{critical}}$ cannot be determined for a particular longitudinal position, the constraint on the lateral position is the centre of the target lane.

rewritten in terms of deviation variable,  $\delta_y$  as:

$$y_{des} - y(k+1) = y_{des} - y(k) - t_s v_y(k) - \frac{t_s^2}{2} a_y(k) - \frac{t_s^3}{6} j_y(k) \quad (3.44)$$

$$\delta_y(k+1) = \delta_y(k) - t_s v_y(k) - \frac{t_s^2}{2} a_y(k) - \frac{t_s^3}{6} j_y(k) \quad (3.45)$$

Similarly, the limits on the lateral position can now be expressed in terms of the deviation variable as:

$$\delta_y(k) \geq \delta_{ymin}(k) \quad (3.46)$$

$$\delta_y(k) \leq \delta_{ymax}(k) \quad (3.47)$$

where  $\delta_{ymax}(k) = y_{des} - y_{min}(k)$  and  $\delta_{ymin}(k) = y_{des} - y_{max}(k)$  respectively.

The lateral motion planning to complete the lane change from an initial point to a desired final point, following the vehicle model and maintaining the constraints can now be written in the form of a standard QP optimisation problem as:

$$\min_z J = \frac{1}{2} z^T H z \quad (3.48)$$

$$s.t. A_{eq} z = B_{eq} \quad (3.49)$$

$$A_{in} z \leq B_{in} \quad (3.50)$$

where  $z = [\delta_y(k), v_y(k), a_y(k), j_y(k)]^T$  and the cost function to be minimised for the control problem is given by:

$$J = \sum_{i=0}^{N-1} (X(i)^T Q X(i) + u(i)^T R u(i)) + X(N)^T P_f X(N) \quad (3.51)$$

where  $X = [\delta_y(k), v_y(k), a_y(k)]^T$  are the states with weight  $Q$  as the stage cost and  $P_f$  as the terminal cost for the final state.  $u = [j_y(k)]$  is the control input to the system with weight  $R$  as the cost. By penalising the deviation from the final desired state ( $\delta_y(N) = 0, v_y(N) = 0, a_y(N) = 0$ ) using high weight values in  $P_f$ , the desired trajectory is derived.



# 4

## Results

In this chapter results from the proposed algorithm are presented. This chapter is structured into two main parts. The first part includes results from each step in the proposed algorithm for an assumed normal behaviour of a traffic environment. The second part is focused on evaluating the proposed algorithm and consists of a series of simulations with different unexpected behaviours of the surrounding vehicles. MATLAB/Simulink is used as the programming tool to simulate and evaluate the different scenarios.

### 4.1 Part A

The lane change traffic environment considers a one-way lane driving scenario where the ego vehicle initially drives in the host lane with no other vehicles in the same lane. The adjacent lane consists of two vehicles, a leading vehicle and a trailing vehicle at all times during the lane change execution. The surrounding vehicles in the adjacent lane are considered to travel with a constant longitudinal velocity and no lateral motion during the entire execution of the manoeuvre. This assumption is used to model the nominal traffic behaviour of the surrounding vehicles. A worse case behaviour different from the nominal behaviour is assumed to force the ego vehicle to initiate an evasive manoeuvre. The general simulation parameters used in this scenario is shown in Table 4.1. The proposed motion planning algorithm consists of four steps as described in Chapter 3 and the results of each step are presented in the following sections.

**Table 4.1:** General simulation parameters for the lane change scenario with a lane change time of 5 seconds and a desired final ego velocity of 18 (m/s)

	Initial Conditions					
	$x_0(m)$	$v_{x0}(m/s)$	$a_{x0}(m/s^2)$	$y_0(m)$	$v_{y0}(m/s)$	$a_{y0}(m/s^2)$
Ego Vehicle	0	16	0	0	0	0
Leading Vehicle	20	18	0	-3.75	0	0
Trailing Vehicle	-20	19	0	-3.75	0	0

### 4.1.1 Critical Zone

Figure 4.1 shows the critical zones plotted around the surrounding vehicles at the start of the lane change manoeuvre. The initial positions of the ego vehicle and the surrounding vehicles are as shown in Table 4.1. The critical zones around the surrounding vehicles at every time instant are calculated based on the predicted nominal motion (constant longitudinal velocity) of the surrounding vehicles throughout the planning horizon. A safe manoeuvre by the ego vehicle is guaranteed by ensuring that the ego vehicle remains outside the critical zones so that a collision free evasive action is possible in the event of any emergency, i.e., leading vehicle crashing or trailing vehicle accelerating.

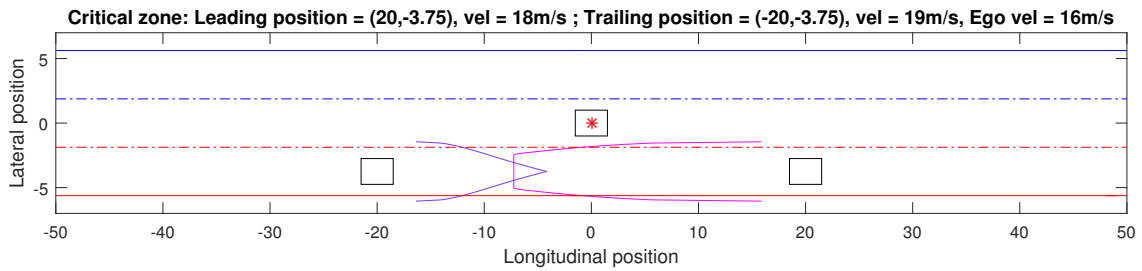


**Figure 4.1:** Critical zones plotted for the initial positions of all occupants in the traffic environment as mentioned in Table 4.1. Ego vehicle, depicted with a red star in the centre, is the only occupant in the initial host lane. The critical zones are predicted with respect to the shown position of the ego vehicle.

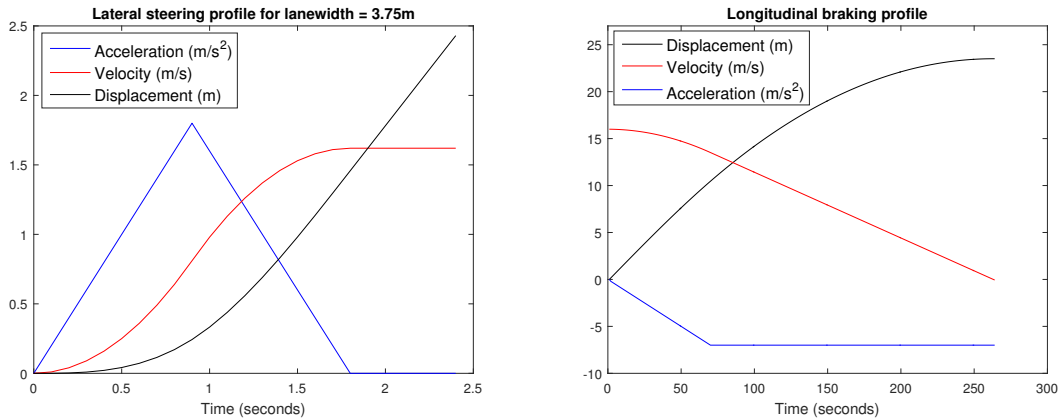


**Figure 4.2:** Lateral and Longitudinal acceleration profiles considered to calculate the critical zone as explained in Section 3.1. *Left:* Lateral acceleration profile considered for the ego vehicle to plan the evasive action by steering. *Right:* Longitudinal deceleration profile considered for the ego vehicle to plan the evasive action by braking.

### 4.1.2 Improvements in lane change efficiency

The constant time gap method discussed in Chapter 2 would require the ego vehicle to maintain a predetermined time gap with respect to the surrounding vehicles before it can even enter the target lane. This would require a high time gap between the vehicles in the adjacent lane for the ego vehicle to initiate a lane change manoeuvre. This approach is very conservative and there is no guarantee that it can always be implemented in dense traffic environment, where the time gap between the surrounding vehicles are relatively less.

In dense traffic scenarios, a more human-like driving behaviour would be to squeeze into gaps available between the surrounding vehicles to show intention for the lane change. This behaviour also gives the opportunity for the ego vehicle to abort the lane change if required. The advantages of the critical zone modelling by factoring in both steering and braking capabilities of the ego vehicle for evasive manoeuvres can be seen in Figure 4.3. The results indicate that sufficient gaps are available in the adjacent lane to show intentions for cases where initiation of lane change would not be possible with the previously discussed constant time gap method. A time gap of around 1.7 seconds between the leading and trailing vehicle in the adjacent lane gives a gap of 1 meter of lateral intrusion for the ego vehicle i.e, for an ego vehicle width of 2 metres, half of the ego vehicle can be positioned within the adjacent lane. This provides the ego vehicle with an opportunity to show intention for lane change and still guarantee safety, thus improving the lane change efficiency.

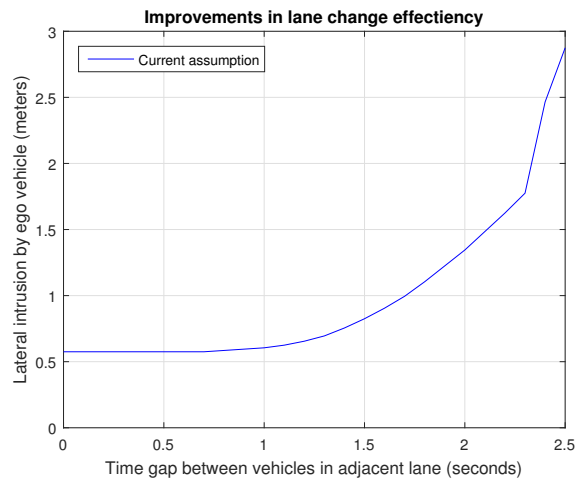


**Figure 4.3:** The lateral intrusion by the critical edge of the ego vehicle into the target lane is plotted against the time gap between the trailing and leading vehicle in adjacent lane. The current assumption is that the lead vehicle can come to crash stop at any instance, and that the trailing vehicle accelerates in order to cut off the lane change manoeuvre. The results are plotted for velocities of ego, trailing and leading vehicle as 18 m/s.

In Figure 4.4, the gap available for lateral intrusion for the ego vehicle is plotted against different velocities of leading and trailing vehicle in adjacent lane for a fixed time gap. The general trend observed is that larger lateral intrusion can be achieved

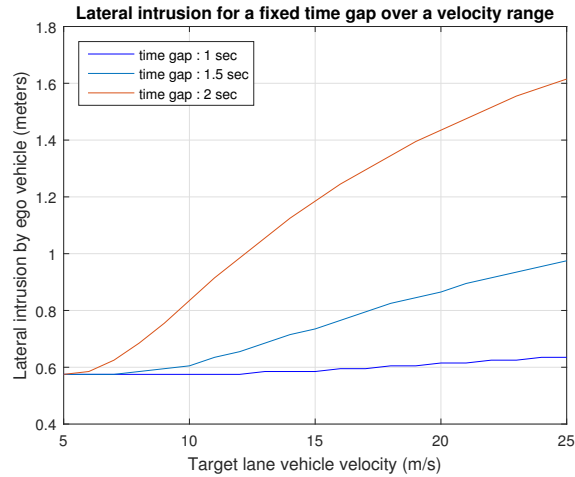


**Figure 4.4:** The lateral intrusion by the critical edge of the ego vehicle into the target lane is plotted against target lane velocity for different time gaps. Both the leading and trailing vehicles in the target lane maintain the same target lane velocity.

at higher velocities. Higher the fixed time gap between the vehicles in the target lane, the greater is the gain in lateral intrusion for increasing target lane velocity. For a fixed time gap between the target lane vehicles, the lane change efficiency is higher at higher velocities.

### 4.1.3 Desired Final Position

The desired final position for the ego vehicle to plan the lane change manoeuvre is calculated based on the predicted motion of the surrounding vehicles at the end of the fixed lane change time. Figure 4.5 shows the predicted positions of the leading vehicle and the trailing vehicle at the end of 5 seconds, which is the fixed lane change time for this scenario. Since the surrounding vehicles are considered to travel with a constant velocity as given in Table 4.1, it can be seen that the distance travelled by the leading and trailing vehicles are 90 and 95 metres respectively. From Figure 4.5, it can also be seen that the critical zones and the region of intersection between the critical zones are different as compared to Figure 4.1 despite the velocities of the surrounding vehicles remaining constant throughout the planning horizon. This is because the critical zones calculated based on the braking or steering capability of the ego vehicle is dependent on the velocity of the ego vehicle and the ego vehicle is considered to have different velocities at the start and end of the lane change manoeuvre in this scenario.

Although the final position of the ego vehicle shown in Figure 4.5 proves to be safe, one can intuitively observe that this is different from a socially acceptable perspective. In real life traffic situations, drivers prefer to end up closer to the leading vehicle at the end of the lane change manoeuvre to position themselves in a lead-follow scenario. However, the method used to model the critical zone around the leading vehicle requires the ego vehicle to maintain this distance in order to initiate an evasive manoeuvre either by steering or braking in case of emergencies.

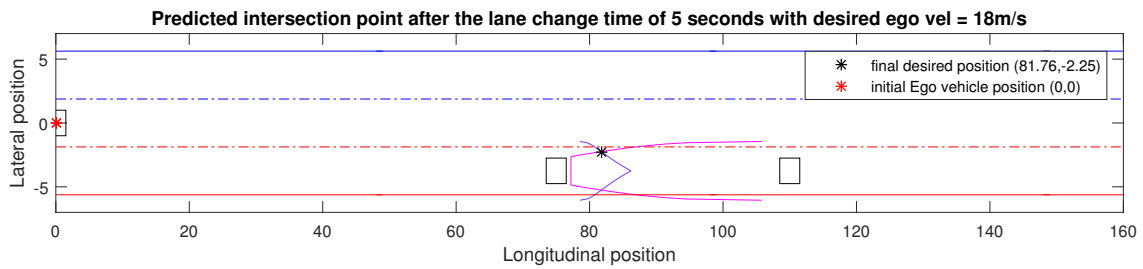


**Figure 4.5:** Desired final position for the ego vehicle calculated based on the intersection of the predicted critical zones at the end of the lane change time.

#### 4.1.4 Longitudinal Motion Planning

The longitudinal motion for the ego vehicle from an initial final position to a desired final position is planned by solving an MPC problem as described in Section 3.3. Figure 4.6 shows the longitudinal position of the ego vehicle and Figure 4.7 shows the velocity and acceleration profile of the ego vehicle over the entire lane change time. From Figure 4.7, it can be seen that the desired final values for the velocity and acceleration are achieved and the profiles remains continuous throughout the planning horizon. The upper and lower limits defining the constraints on the longitudinal velocity used for this case are  $0 \text{ m/s}$  and  $30 \text{ m/s}$  respectively. Similarly, the constraints used on the longitudinal acceleration are  $-7 \text{ m/s}^2$  and  $+7 \text{ m/s}^2$  and that for the longitudinal jerk are  $-10 \text{ m/s}^3$  and  $+10 \text{ m/s}^3$ . These parameters are considered based on how severe the evasive manoeuvre should be. In case of a more hard evasive manoeuvre, higher values on the jerk and acceleration can be considered.

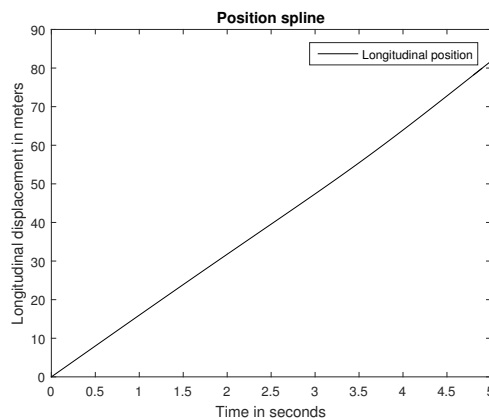


**Figure 4.6:** Longitudinal Position of the ego vehicle planned over the entire lane change time of 5 seconds.

## 4. Results

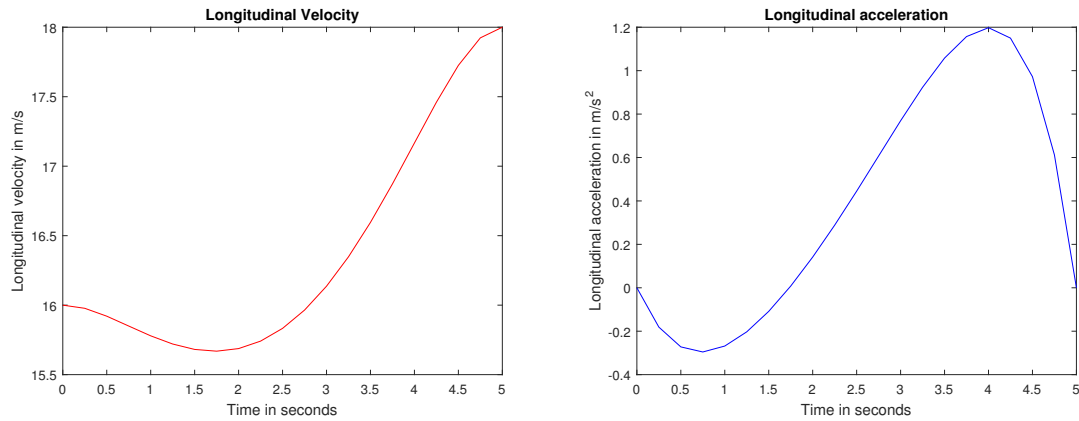


**Figure 4.7:** *Left:* Velocity profile of the ego vehicle for the planned longitudinal motion with an initial velocity of 16 m/s and final desired velocity of 18m/s. *Right:* Acceleration profile of the ego vehicle for the planned longitudinal motion with an initial and final desired value of 0m/s<sup>2</sup>.

### 4.1.5 Lateral Motion Planning

As described in Section 3.4, the lateral motion for the ego vehicle is planned by solving the formulated QP problem using Model Predictive Control. Since a safe motion is guaranteed by ensuring that the ego vehicle stays outside the critical zone of the surrounding vehicle at every instant of the planning, the constraints on the lateral position are calculated from the predicted critical zones during the entire planning horizon. This gives the ego vehicle the possibility to execute the evasive action in case of emergencies. Figure 4.8 shows the lateral position of the ego vehicle and Figure 4.9 shows the lateral velocity and acceleration profile of the ego vehicle over the entire lane change time.

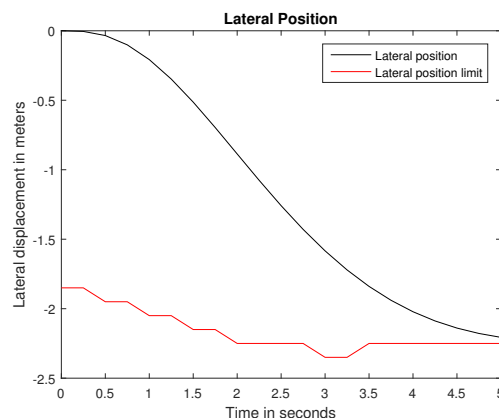


**Figure 4.8:** Lateral Position of the ego vehicle planned over the entire lane change time of 5 seconds.

Similar to the constraints used for the longitudinal motion planning, the lateral motion is also subjected to constraints. The constraints used for the simulation are

are  $-1 \text{ m/s}$  and  $+1 \text{ m/s}$  for the lateral velocity,  $-2 \text{ m/s}^2$  and  $+2 \text{ m/s}^2$  for the lateral acceleration and  $-2 \text{ m/s}^3$  and  $+2 \text{ m/s}^3$  for the lateral jerk respectively. As in case of the longitudinal motion planning, to obtain a more hard evasive manoeuvre higher values on the jerk and acceleration can be considered.

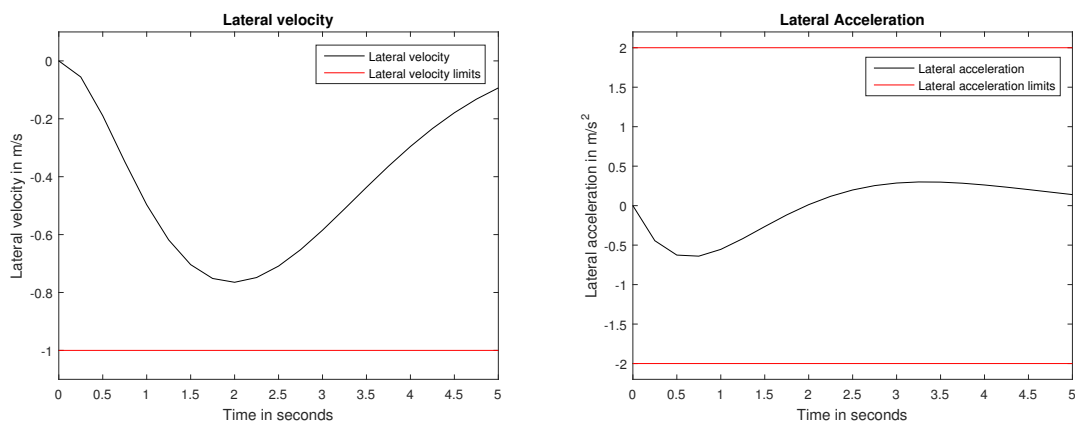
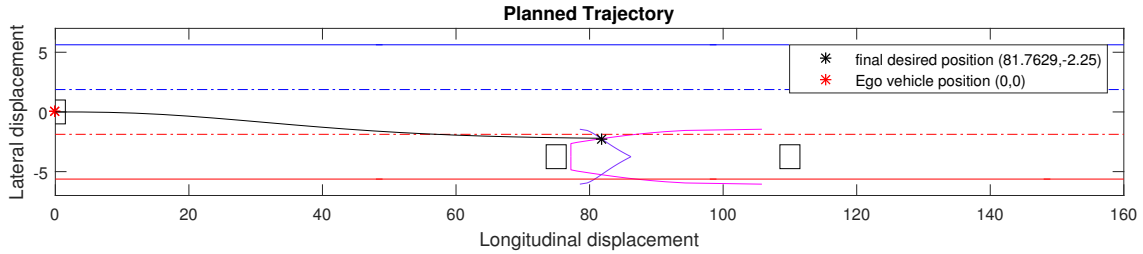
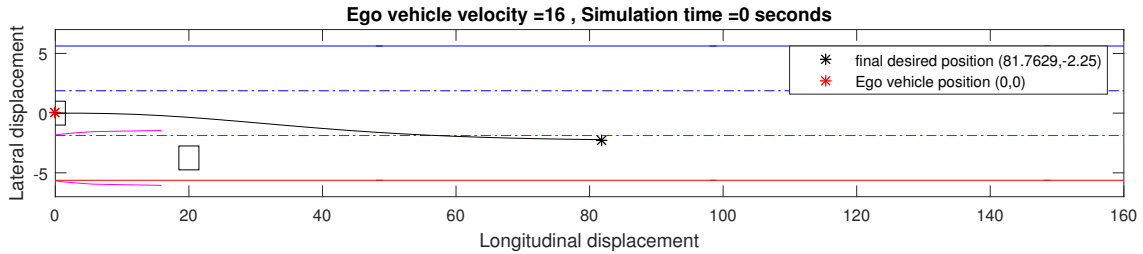


**Figure 4.9:** *Left:* Velocity profile of the ego vehicle for the planned lateral motion. *Right:* Acceleration profile of the ego vehicle for the planned lateral motion.

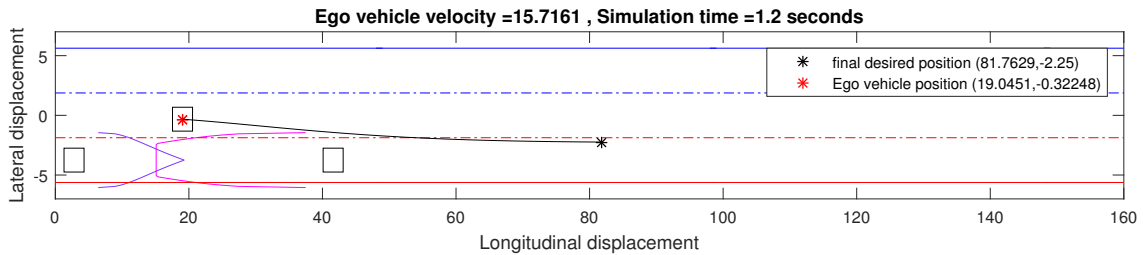
### 4.1.6 Simulation of the planned trajectory



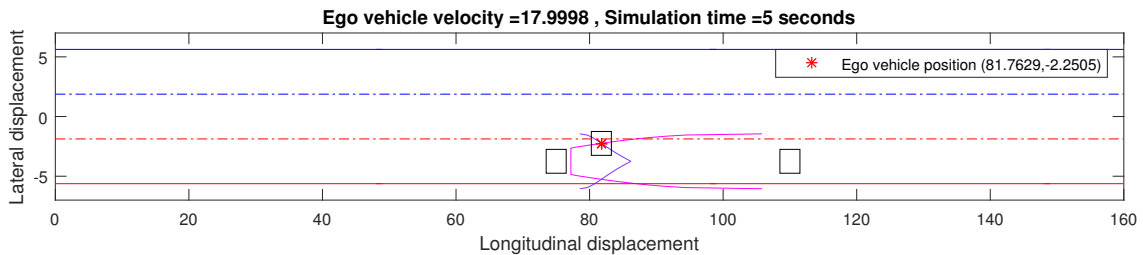
(a) Predicted critical zones at the end of the lane change time and the planned lane change trajectory shown from the start to the end of lane change time.



(b) Planned lane change trajectory at the start of simulation time. Initial position of the ego vehicle is at (0,0).



(c) Traffic environment when simulation time is 1 second. Ego vehicle follows the planned lane change trajectory.



(d) Completion of lane change manoeuvre with the proposed motion planning algorithm. Ego vehicle has positioned itself in the gap between the two surrounding vehicles without compromising the possibility to initiate an evasive action in the event of an emergency.

**Figure 4.10:** Simulation of the proposed motion planning algorithm in a traffic scenario where ego vehicle has to leave its host lane and position itself in the adjacent lane between the two surrounding vehicles.

The proposed lane change motion planning algorithm is then evaluated for the complete motion in the traffic scenario as explained in the beginning of this section. The ego vehicle has to position itself in the gap between the two surrounding vehicles in the adjacent lane with the ability to perform an evasive manoeuvre in case of emergencies. Figure 4.10 shows the simulation of the proposed lane change algorithm at some selected time instances in the considered scenario.

## 4.2 Part B

In this section, the proposed motion planning algorithm is evaluated by simulating a series of traffic scenarios where the surrounding vehicles in the target lane execute behaviours which require the ego vehicle to perform an evasive manoeuvre. For example, scenarios where the leading vehicle in the adjacent lane comes to an immediate stop (crash) or the trailing vehicle accelerating at the end of the lane change. A scenario where the trailing vehicles accelerates during the lane change is also looked into. This is to verify the robustness of the algorithm against prediction errors and the ability to abort the lane change manoeuvre.

### 4.2.1 Case 1 - Ego vehicle steers to avoid collision

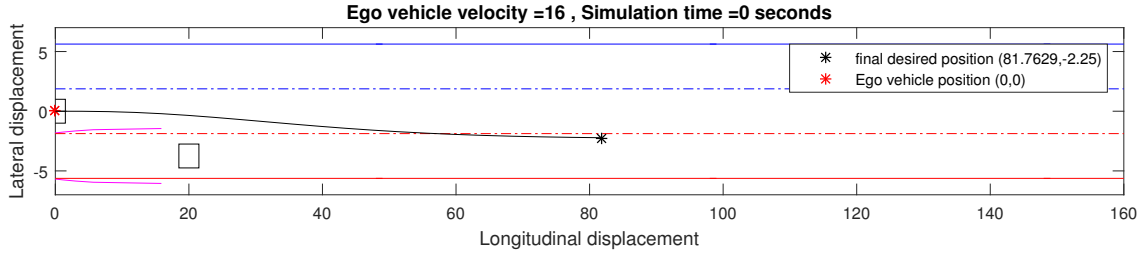
In this case, two scenarios referred as Scenario 1 and Scenario 2 are considered to evaluate the proposed planning algorithm. In both the scenarios, the ego vehicle is required to steer away in order to avoid a collision. In both the scenarios, a fixed lane change time of 5 seconds is considered for the ego vehicle. The ego vehicle drives in an initial host lane where it is the only occupant and there are two surrounding vehicles - a leading vehicle and a trailing vehicle in the adjacent target lane. The initial conditions for both the scenarios are shown in Table 4.2. In Scenario 1, the leading vehicle is considered to stop immediately at the end of the lane change time. The ego vehicle is then required to perform the evasive action in order to not collide with the leading vehicle. In Scenario 2, the trailing vehicle is considered to accelerate at the end of the lane change time at a constant acceleration of  $2 \text{ m/s}^2$ . In both the scenarios the surrounding vehicles are considered to have a constant longitudinal velocity until the end of lane change time.

Figure 4.11 shows the results from the simulation of Scenario 1 and Figure 4.13 shows the results from Scenario 2. The lateral velocity and lateral acceleration profiles of the ego vehicle during the entire lane change manoeuvre and the evasive manoeuvre is presented in Figure 4.12. From Figure 4.12, it can be seen that the lateral velocity and the lateral acceleration is  $0 \text{ m/s}$  and  $0 \text{ m/s}^2$  respectively at the start and end of the lane change manoeuvre as well as the evasive manoeuvre. This ensures that the ego vehicle stays within the respective lane at the end of each manoeuvre.

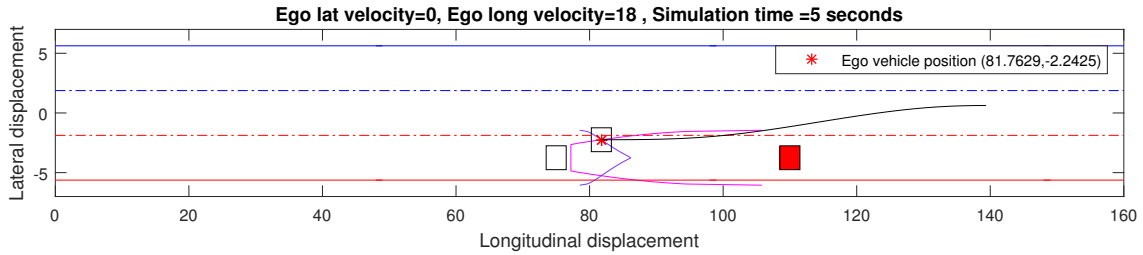
## 4. Results

**Table 4.2:** General parameters for the lane change scenario with a lane change time of 5 seconds and a desired final ego velocity of 18 (m/s)

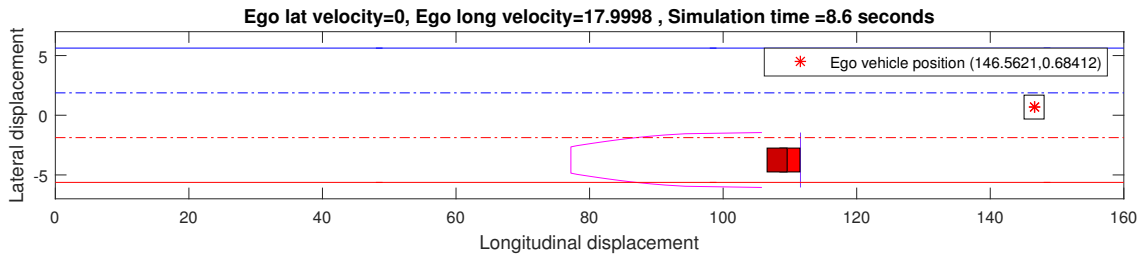
	Initial Conditions					
	$x_0(m)$	$v_{x0}(m/s)$	$a_{x0}(m/s^2)$	$y_0(m)$	$v_{y0}(m/s)$	$a_{y0}(m/s^2)$
Ego Vehicle	0	16	0	0	0	0
Leading Vehicle	20	18	0	-3.75	0	0
Trailing Vehicle	-20	0	-3.75	0	0	



(a) Planned lane change trajectory at the start of simulation time. Initial position of the ego vehicle is at (0,0). Lane change trajectory shown in black connecting the initial and the final positions.



(b) Simulation result at the end of lane change completion time (5 seconds). Ego vehicle has positioned itself in the gap between the two surrounding vehicles. Leading vehicle crash shown in red and the ego vehicle's evasive motion represented in the black trajectory.



(c) Simulation result when ego vehicle has completed the evasive action by steering away to avoid collision.

**Figure 4.11:** *Scenario 1:* Lane change scenario where the leading vehicle comes to an immediate stop at the end of lane change time. The ego vehicle steers away to avoid collision with the leading vehicle.

It should be noted that in both the scenarios, *Scenario 1* and *Scenario 2*, the ego vehicle steers away with the assumed profile to avoid a collision. Also in both the

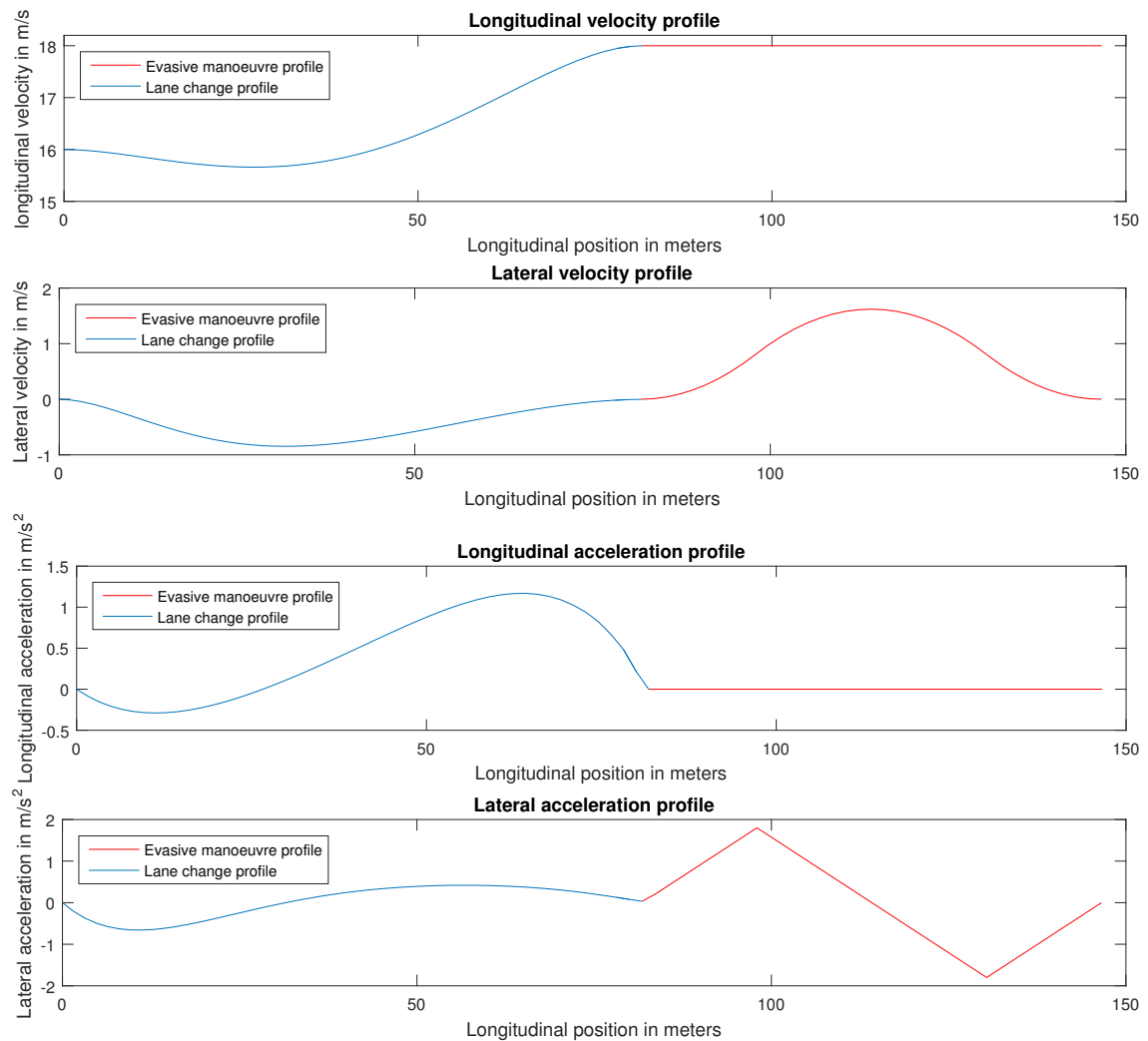
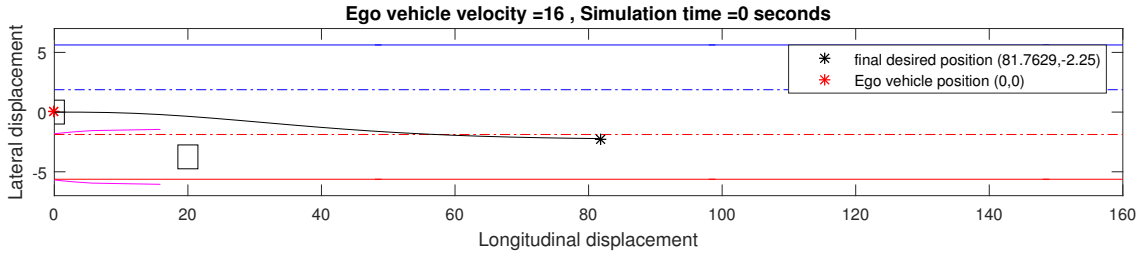


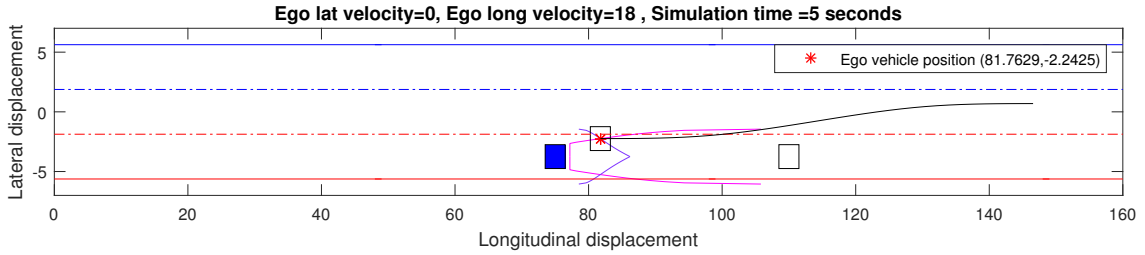
**Figure 4.12:** Longitudinal and Lateral velocity and acceleration profile of the Ego vehicle in *Scenario 1*. In this scenario, the ego vehicle steers away to avoid a collision.

scenarios, the position of the ego vehicle when it initiates the evasive manoeuvre remains the same, and the behaviour of the surrounding vehicle changes. Therefore, the acceleration and velocity profiles of the ego vehicle remains the same in both the scenarios and is as shown in Figure 4.12.

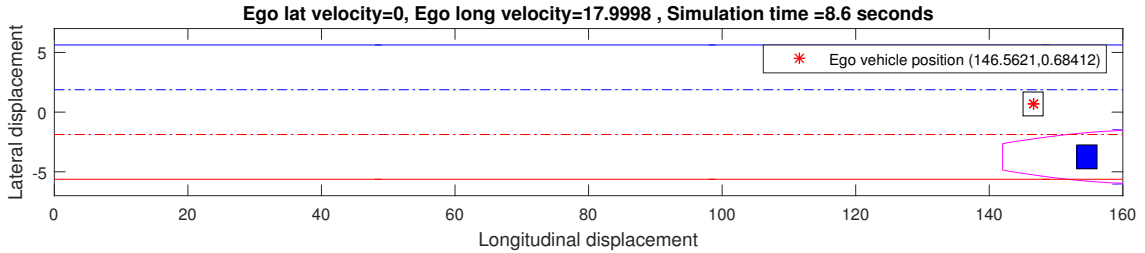
## 4. Results



(a) Planned lane change trajectory at the start of simulation time. Initial position of the ego vehicle is at (0,0). Lane change trajectory shown in black connecting the initial and the final positions.



(b) Simulation result at the end of lane change completion time (5 seconds). Ego vehicle has positioned itself in the gap between the two surrounding vehicles. Trailing vehicle acceleration shown in blue and the ego vehicle's evasive motion represented in the black trajectory.



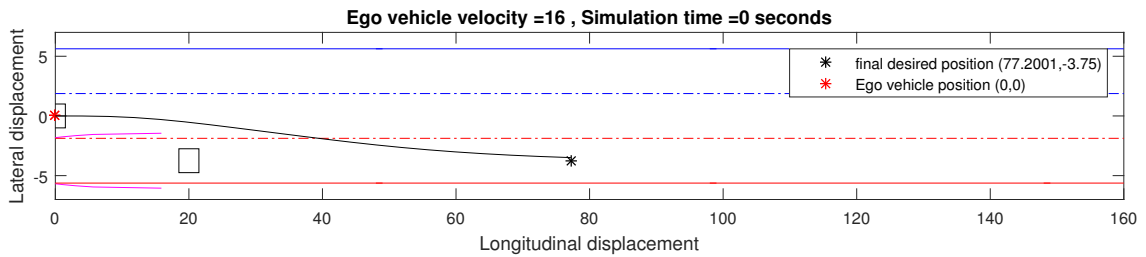
(c) Simulation result when ego vehicle has completed the evasive action by steering away to avoid collision.

**Figure 4.13:** *Scenario 2:* Lane change scenario where the trailing vehicle accelerates with a constant acceleration of  $2 \text{ m/s}^2$  at the end of lane change time. The ego vehicle steers away to avoid collision.

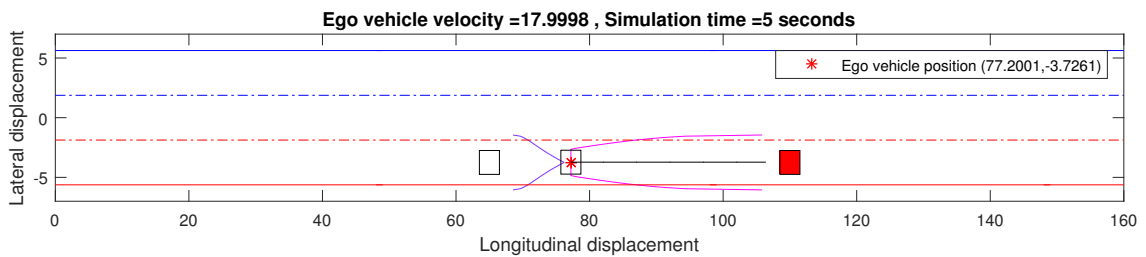
### 4.2.2 Case 2 - Ego vehicle brakes to avoid collision

In this case, a scenario referred as Scenario 3 is considered to evaluate the capability of the ego vehicle to brake in order to avoid collision. The traffic environment and the initial conditions in Scenario 3 are similar to that present in Scenario 1. In Scenario 3 also, the leading vehicle comes to an immediate stop at the end of the lane change time similar to Scenario 1. However, the motion planning algorithm in this case results in a motion where the ego vehicle can position itself in the centre of the target lane by the end of the lane change time. In this case, since the ego vehicle is at a position where  $T_{\text{steer}} > T_{\text{brake}}$  (refer (3.19)), the only evasive action possible for the ego vehicle to avoid collision is to initiate braking. Figure 4.14 shows the results

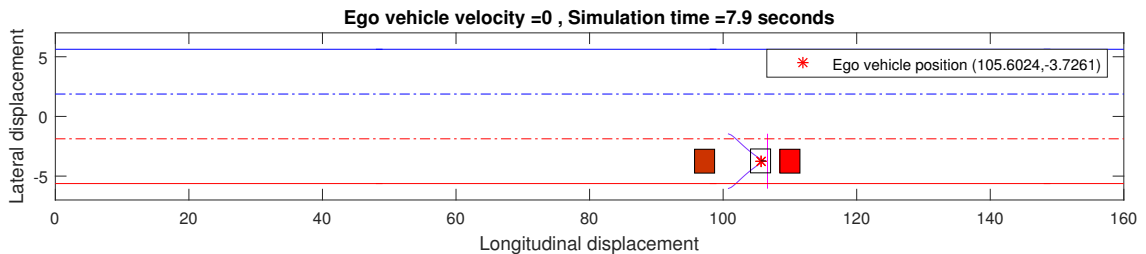
from the simulation of Scenario 3 and Figure 4.15 shows the longitudinal velocity and longitudinal acceleration profiles of the ego vehicle throughout the simulation. From Figure 4.15, it can be seen that the ego vehicle initiates braking with the assumed braking profile as shown in 4.2 during the evasive manoeuvre and the longitudinal velocity reaches zero to avoid a collision.



(a) Planned lane change trajectory at the start of simulation time. Initial position of the ego vehicle is at (0,0). Lane change trajectory shown in black connecting the initial and the final positions.



(b) Simulation result at the end of lane change completion time (5 seconds). Ego vehicle has positioned itself in the adjacent lane. Leading vehicle crash shown in red and the ego vehicle's evasive motion represented in the black trajectory.



(c) Simulation result when ego vehicle has completed braking to avoid collision with the leading vehicle.

**Figure 4.14:** *Scenario 3:* Lane change scenario where the leading vehicle comes to an immediate stop at the end of lane change time. The ego vehicle brakes to avoid collision with the leading vehicle.

### 4.2.3 Case 3 - Ego vehicle plans a new path to get back to host lane

In Case 3, the proposed motion planning algorithm is evaluated for a scenario where the behaviour of the surrounding vehicle does not match the prediction assumptions.

## 4. Results

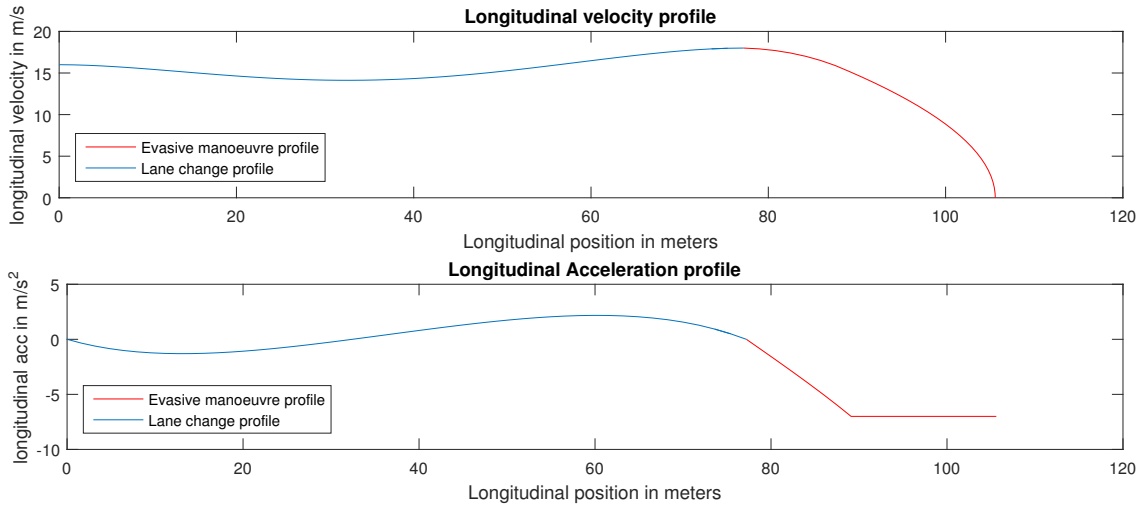
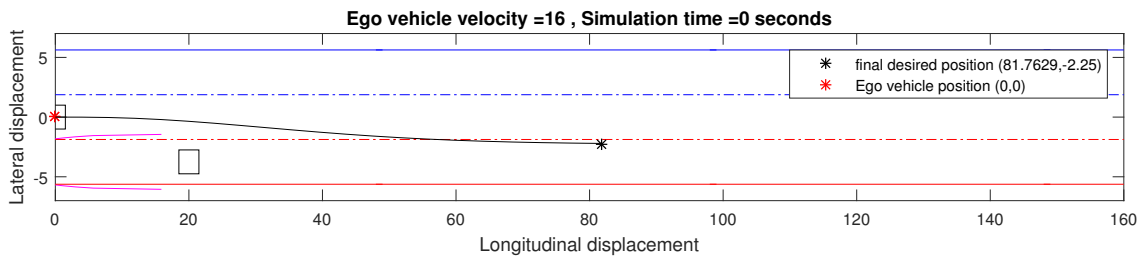
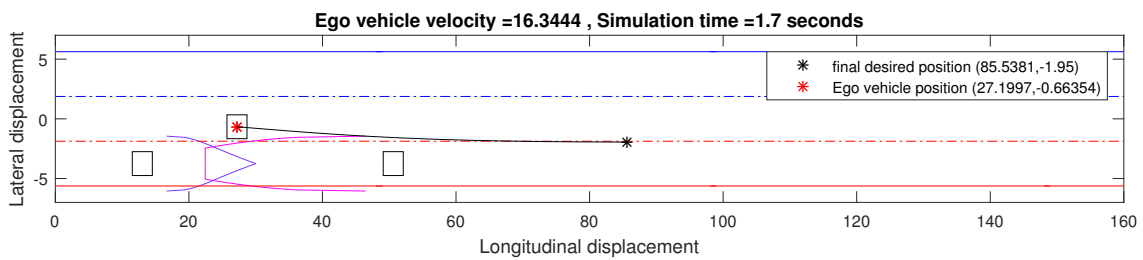


**Figure 4.15:** *Top:* Longitudinal velocity profile of the ego vehicle in *Scenario 3*. *Bottom:* Longitudinal acceleration profile of the ego vehicle in *Scenario 3*

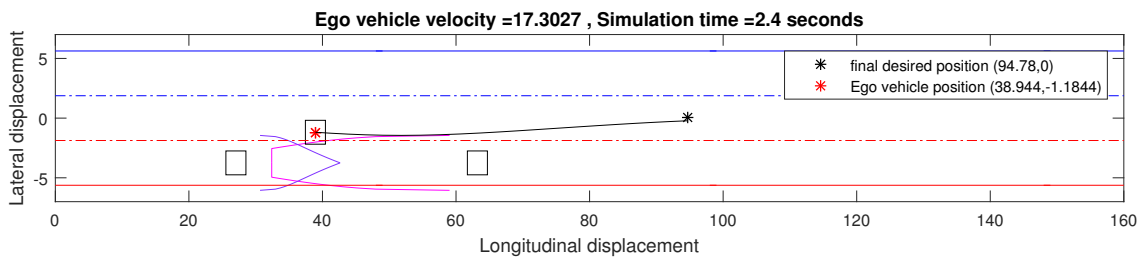
This scenario referred as *Scenario 4* shows that the proposed motion planning algorithm is capable of handling prediction errors during the lane change planning. In *Scenario 4*, the traffic environment and the initial conditions are similar to *Scenario 2*. However, instead of the trailing vehicle accelerating with a constant acceleration at the end of the lane change time, in this scenario the trailing vehicle accelerates at  $0.5 \text{ m/s}^2$  during the course of the lane change performed by the ego vehicle. As a result of this behaviour, the predictions made for the critical zone at the end of lane change time (i.e., 5 seconds) using a constant longitudinal velocity motion becomes invalid. However since the algorithm re-plans the entire motion with every instant, it is possible to account for this behaviour with every new data received. Figure 4.16 shows the results of the proposed planning algorithm in this scenario. From Figure 4.16, it can be seen that the final position to which the lane change is planned keeps changing to account for changes in the behaviour of the surrounding vehicles. When the lane change manoeuvre becomes infeasible for the ego vehicle to position itself in the adjacent lane, a new motion plan is done to position the ego vehicle in the centre of the initial host lane. Figure 4.17 shows the lateral and longitudinal velocity profile of the ego vehicle during the entire manoeuvre in *Scenario 4*.



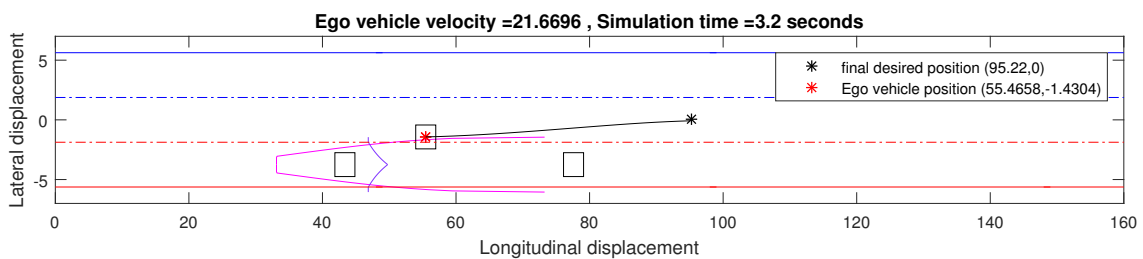
(a) Planned lane change trajectory at the start of simulation time. Initial position of the ego vehicle is at (0,0). Lane change trajectory shown in black connecting the initial and the final positions.



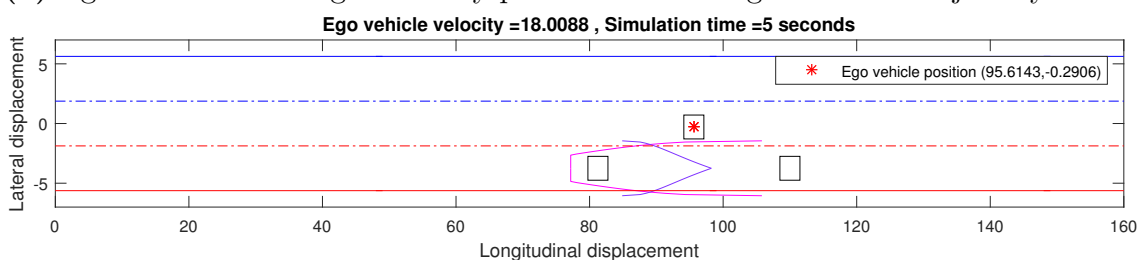
(b) Simulation result after 1 second. Trailing vehicle is considered to travel with a constant acceleration of  $0.5 \text{ m/s}^2$ . Final desired position changed as compared to the above result as the critical zone at the end of lane change time is now predicted using the new data.



(c) New trajectory planned to abort the lane change manoeuvre and position the ego vehicle back in the initial lane. The lane change abortion trajectory planned is shown in black.



(d) Ego vehicle following the newly planned lane change abortion trajectory.



(e) Simulation result at the completion of the scenario. The ego vehicle has positioned itself at the centre of the initial lane.

**Figure 4.16:** *Scenario 4:* Lane change scenario where the trailing vehicle accelerates during the ego vehicle's lane change manoeuvre. The algorithm is used to generate a new motion plan for the ego vehicle to get back to the initial host lane.

## 4. Results

---

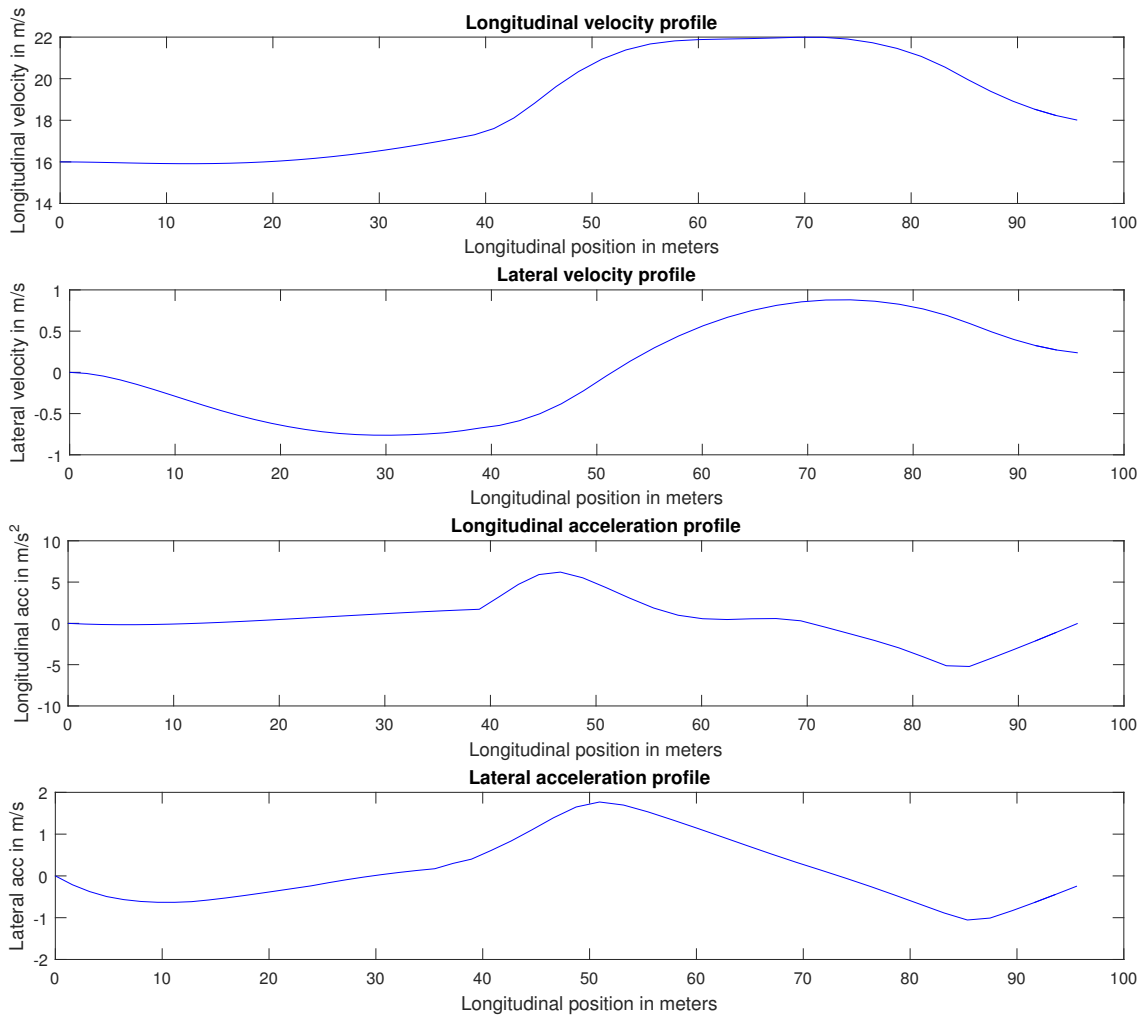


**Figure 4.17:** Longitudinal and Lateral velocity and acceleration profile of the Ego vehicle in *Scenario 4*. In this scenario, the behaviour of the surrounding vehicles does not match the assumptions used for path prediction.

# 5

## Discussions

This chapter includes discussions about the performance of the proposed algorithm under conditions different from the current assumptions used in the modelling. First section discusses the performance of the algorithm with respect to information available about the surrounding vehicles. It is then followed by a brief discussion on the algorithm when the bicycle model is used to model the vehicle motion. The chapter is concluded with the final section discussing about an analytical solution for motion planning.

### 5.1 Performance with different assumptions about surrounding vehicles

The assumption that the leading vehicle crashes to a stop in the next instant is not very realistic and very conservative. If more information about the surrounding environment is available such that the worst case assumption of the leading vehicle can be altered, a better performance can be achieved.

In figure 5.1, lane change performance for a new worst case assumption for the leading vehicle can be seen. The new worst case assumption is that the leading vehicle crashes to another vehicle of equal mass, which effectively reducing its velocity immediately by half before coming to a stop. This is a less conservative assumption and it gives better performance. For a time gap of 2 seconds between the leading and trailing vehicle in the adjacent lane the ego vehicle can effectively manoeuvre into the centre of target lane during lane change, and it only needs a time gap of around 1.25 seconds to intrude half of its width laterally.

This analysis gives a clear picture about the effect of the worst case assumptions on the lane change performance efficiency. Having better sensor information about the surrounding environment will help in formulating less conservative worst-case scenarios while not compromising on safety. For example, if the vehicle in front of the leading vehicle could be observed the worst case scenario will be that the vehicle in front of the leading vehicle comes to an immediate stop at any instance. This will reduce the critical zone around the leading vehicle considerably.

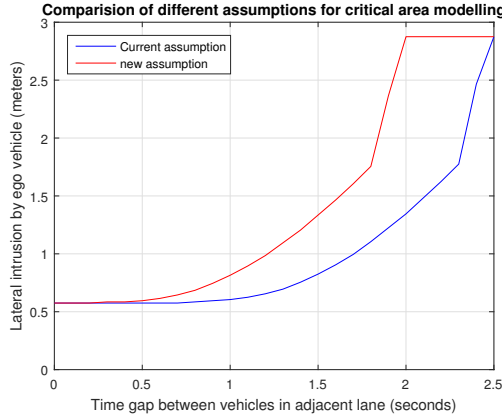


**Figure 5.1:** The lateral intrusion by the critical edge of the ego vehicle into the target lane is plotted against the time gap between the trailing and leading vehicle in adjacent lane. The blue curve shows the gain with the current assumption and the red curve shows the gain with the change in assumptions about the surrounding vehicles. The results are plotted for velocities of ego, trailing and leading vehicle as 18 m/s.

## 5.2 Different motion models

Throughout the modelling and planning of the proposed algorithm, the point mass vehicle model is used to model the critical zones and the motion of the vehicles. However, there are other motion models available namely the one track model and the two track model which can be used in the modelling of the critical zone and the vehicle motion. The performance of the proposed algorithm with the bicycle model is discussed in this section.

### 5.2.1 Bicycle model

The bicycle model, also known as the single track model can be described considering the longitudinal ( $x$ ), lateral ( $y$ ) and yaw ( $\psi$ ) motion of the vehicle under different assumptions. This section describes the linear bicycle model for lateral vehicle dynamics with two degrees of freedom, which is often simplified by projecting the front and the rear wheels on two virtual wheels and the use of linearised equations. The two degrees of freedom are represented by the lateral position ( $y$ ) and the yaw angle ( $\psi$ ). The model described is represented in Figure 5.2 based on [24]. Using Newton's second law and considering that only the front steering angle  $\delta_f$ , the equations describing the lateral motion can be obtained as

$$m(\ddot{y} + v_x \dot{\psi}) = F_{yf} \cos \delta - F_{xf} \sin \delta + F_{yr} \quad (5.1)$$

$$I_z \ddot{\psi} = L_f (F_{yf} \cos \delta - F_{xf} \sin \delta) - L_r F_{yr}. \quad (5.2)$$

Furthermore, assuming that the steering angle  $\delta$  is small and neglecting the influence

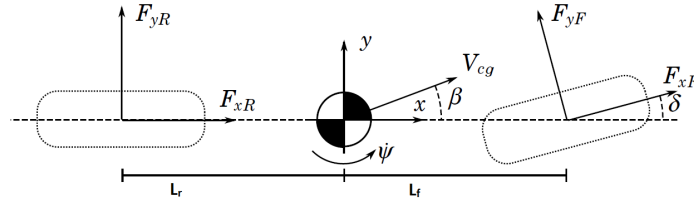


**Figure 5.2:** Single-track model, showing the combined front and rear tire forces, the steering angle  $\delta$ , the yaw rate  $\dot{\psi}$ , and the vehicle side-slip angle  $\beta$ .

of the longitudinal force  $F_{xf}$  [23], the model can be simplified as:

$$\ddot{y} = \frac{F_{yf}}{m} + \frac{F_{yr}}{m} - v_x \dot{\psi} \quad (5.3)$$

$$\ddot{\psi} = \frac{L_f}{I_z} F_{yf} - \frac{L_r}{I_z} F_{yr} \quad (5.4)$$

where  $F_{yf}$  and  $F_{yr}$  are the front and rear lateral tire forces respectively,  $I_z$  is the moment of inertia about the  $z$  axis,  $v_x$  is the constant longitudinal velocity,  $L_f$  and  $L_r$  are the distances from the front and rear wheels to the centre of gravity respectively.

The slip angle of a tire is defined as the angle between the orientation of the tire and the orientation of the velocity vector of the wheel and therefore the slip angles for the front and rear wheels,  $\alpha_f$  and  $\alpha_r$  are given by:

$$\alpha_f = \frac{\dot{y} + L_f \dot{\psi}}{v_x} - \delta \quad (5.5)$$

$$\alpha_r = \frac{\dot{y} - L_r \dot{\psi}}{v_x}. \quad (5.6)$$

For a linear tire model with very small slip angles, the lateral tire forces can be approximated as

$$F_{yf} = -C_{\alpha f} \alpha_f \quad (5.7)$$

$$F_{yr} = -C_{\alpha r} \alpha_r. \quad (5.8)$$

where  $C_{\alpha f}$  and  $C_{\alpha r}$  are the cornering stiffness coefficients for the front and rear tires respectively.

As the longitudinal velocity  $v_x$  is assumed to be constant, a linear and time invariant two degree of freedom bicycle model for lateral vehicle dynamics can be obtained by considering the lateral velocity  $\dot{y}$  and yaw rate  $\dot{\psi}$  as the states and the steering angle  $\delta$  as the input. The state space form is given as:

$$\begin{bmatrix} \ddot{y} \\ \ddot{\psi} \end{bmatrix} = \begin{bmatrix} -\frac{C_{\alpha f} + C_{\alpha r}}{m v_x} & \frac{L_r C_{\alpha r} - L_f C_{\alpha f}}{m v_x} - v_x \\ \frac{L_r C_{\alpha r} - L_f C_{\alpha f}}{I_z v_x} & -\frac{L_r^2 C_{\alpha r} + L_f^2 C_{\alpha f}}{I_z v_x} \end{bmatrix} \begin{bmatrix} \dot{y} \\ \dot{\psi} \end{bmatrix} + \begin{bmatrix} \frac{C_{\alpha f}}{m} \\ \frac{L_f C_{\alpha f}}{I_z} \end{bmatrix} [\delta]. \quad (5.9)$$

### 5.2.2 Comparison of different vehicle models in critical zone modelling

The critical zone will vary for different vehicle models under consideration. Figure 5.3 shows critical zone for both pointmass and bicycle model. It has to be noted that  $T_{brake}$  stays unaffected by the choice of models, while  $T_{steer}$  depends on the vehicle model.  $T_{steer}$  for the bicycle model shown in the figure is calculated for initial heading angle of zero.

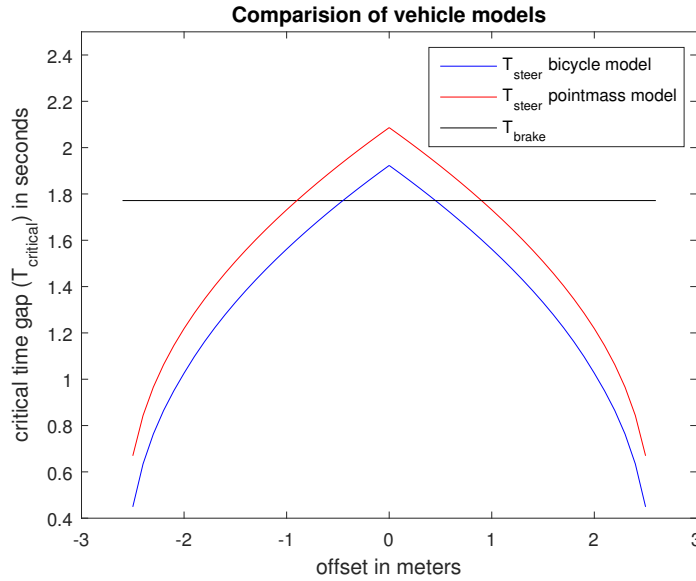


**Figure 5.3:** Critical time gap plotted as a function of offset in the target lane for both pointmass and bicycle model

It can be seen that the point mass model is more conservative than the bicycle model, while not compromising on safety. The pointmass model is simpler to implement, whereas bicycle model is more accurate as a vehicle model for a car. The current thesis work was completed using pointmass model since it was simpler to implement and it did not compromise on safety. A more accurate vehicle model can be implemented and evaluated instead of pointmass model as future work.

## 5.3 Analytical solutions for motion planning

The motion planning method discussed in this thesis is based on Model Predictive Control approach. Although no investigations have been carried out as a part of this thesis on the real time performance of this approach in an autonomous vehicle, there are various works in literature which discuss the computational efficiency of an MPC approach for autonomous motion planning. There are also different methods employed for solving motion planning problems. The different methods are discussed in detail in [17]. One of the computationally efficient method in motion planning is

to determine an analytical solution connecting two points which in this case are the initial point in the host lane and the desired final point in the adjacent target lane.

The longitudinal path planning proposed is based on [26], which is a proprietary path planning algorithm developed by Volvo. The longitudinal trajectory problem is formulated to find a two segment spline to connect two points with constraints on position  $x$ , velocity  $v_x$ , acceleration  $a_x$  and jerk  $j_x$  by utilising the boundary conditions at the start and end of the trajectory. A fifth degree polynomial is used to formulate the position in order to have smooth transition for velocity, acceleration and jerk as jerk is the third differentiation of position. The advantage of this simple path planning method is the real time capability as it is less computationally expensive due to the existence of an analytical expression. The boundary constraints defined at the start time  $t = 0$ , and the final time  $t_f$  when the lane change is complete, are as follows:

$$\begin{aligned}
 x(0) &= 0 & x(t_f) &= x_{des} \\
 v_x(0) &= v_x & v_x(t_f) &= v_{des} \\
 a_x(0) &= 0 & a_x(t_f) &= 0 \\
 j_x(0) &= 0 & j_x(t_f) &= 0
 \end{aligned} \tag{5.10}$$

where  $x_{des}$  is the desired final position given by  $X_{Intersect}$  calculated as described in the previous section.  $v_{des}$  is the desired final velocity. With the above mentioned boundary conditions, the two quintic (fifth degree) polynomial expressions for the two segment spline with one knot in between is generated based on spline type 1 as described in [26] where the RMS value of the jerk is minimised.



# 6

## Conclusion

In this thesis, the problem of autonomous motion planning was studied. A novel method for motion planning of autonomous lane change manoeuvre in complex traffic environment with the ability to abort is proposed. The proposed lane change planning algorithm has the following characteristics:

- **Suitable for dense urban traffic environments**

The proposed algorithm makes use of the ability of the ego vehicle to either brake or steer in order to avoid a collision. This has been considered in determining the critical zone around the vehicles also in the motion planning throughout the manoeuvre. A simple method of finding the safest position in the target lane is proposed. With the combination of these features and the ability to execute an evasive action at any point of the manoeuvre, results show that the proposed algorithm can be used for autonomous lane change in dense traffic environments.

- **Robust and Safe**

The safety of the planned manoeuvre was guaranteed by ensuring that the ego vehicle remains outside the critical zone thereby having the possibility to execute an evasive action in case of emergencies.

- **Feasible**

The models and the constraints used in the motion planning algorithm takes into account limitations of the vehicle.

In the proposed algorithm, the trajectory from the initial to the final point for the lane change manoeuvre was determined independently for lateral and longitudinal direction. This ensured that the desired final position, velocity and acceleration in both the lateral and the longitudinal direction, was achieved without violating the critical zone at the end of lane change time. The lane change manoeuvre and the evasive manoeuvres was tested and evaluated through a series of simulations replicating different traffic behaviours. The algorithm was found to give satisfying results with respect to its characteristics

### 6.1 Future work

The proposed motion planning algorithm has been evaluated in simulation environment by stimulating worst case traffic scenarios. As a continuation of the work done in this thesis, the proposed algorithm can be extended for experimental validation in real traffic scenarios by implementing in an autonomous vehicle.

Point mass vehicle model is used in all steps of the proposed motion planning algorithm. Although the modelling of the critical zone using a bicycle model is discussed, the performance of the algorithm using the bicycle model for different traffic scenarios are not evaluated. The proposed algorithm can be used with other vehicle models like the bicycle model and two track model and the performance with more accurate models can be compared to the existing solution. This can give a clear picture on the improvement in lane changing efficiency using more complex vehicle models.

The surrounding vehicles in the traffic scenarios simulated in this thesis are considered to have zero lateral movement. While this is an assumption that can simplify the problem, it cannot be considered true for all traffic environments. The proposed algorithm can be extended to include the possibility to include lateral movement of the surrounding vehicles.

The modelling of the critical zone around vehicles in the host lane are discussed in Chapter 3. The simulations carried out to evaluate the performance of the algorithm however do not include vehicles in the host lane. Including vehicles in the host lane introduces additional constraints on the lateral and the longitudinal position of the ego vehicle and the proposed algorithm can still be used to plan a lane change manoeuvre without entering the critical zones. It should also be noted that when vehicles in the host lane are included, care should be taken in planning the evasive manoeuvre which takes the ego vehicle back to the original lane in case of any worst case traffic situation.

# Bibliography

- [1] Frisk, D. (2015) A Chalmers University of Technology Master's thesis template for L<sup>A</sup>T<sub>E</sub>X. Unpublished.
- [2] Global Status Report on Road Safety, *World Health Organization*, 2015.
- [3] Social costs of accidents in Sweden, *Swedish Civil Contingencies Agency*, December 2012
- [4] Road Safety Annual Report 2014, *International Traffic Safety Data and Analysis Group*
- [5] Traffic Safety Facts, *National Highway Traffic Safety Administration*, Research Note, March 2016.
- [6] Dödade och svårt skadade personer i polisrapporterade vägtrafikolyckor fördelade efter olyckstyp 1985-2008 (Statistics on road traffic accidents in Sweden 1985-2008)
- [7] The Economic and Societal Impact of Motor Vehicle Crashes, 2010 (Revised), *National Highway traffic Safety Administration*, May 2015(Revised).
- [8] Todd Litman. *Autonomous Vehicle Implementation Predictions: Implications for Transport Planning*. Victoria Transport Policy Institute, December 2015.
- [9] Isaac Asher. *Towards an Autonomous World: Making sense of the Potential Impacts of Autonomous Vehicles*, Georgia Institute of Technology, May 2014.
- [10] McKinsey&Company, *Ten ways autonomous driving could redefine the automotive world*. Retrieved May 2016 from <<http://www.mckinsey.com/industries/automotive-and-assembly/our-insights/ten-ways-autonomous-driving-could-redefine-the-automotive-world>>.
- [11] SAE International, *Levels of Driving Automation defined in New SAE International Standard J3016*. Retrieved May 2016 from <[http://www.sae.org/misc/pdfs/automated\\_driving.pdf](http://www.sae.org/misc/pdfs/automated_driving.pdf)>
- [12] Preliminary statement of policy concerning automated vehicles, *National Highway traffic Safety Administration*, 2013.
- [13] Will Knight, *Driverless Cars Are Further Away Than You Think*. MIT Technology Review, October 2013. Retrieved May 15, 2016 from <<https://www.technologyreview.com/s/520431/driverless-cars-are-further-away-than-you-think/>>

- [14] Chuck Tannert, *Our Ultimate Driverless Car Report Card*. Fascompany. Retrieved May 15, 2016 from <<http://www.fastcompany.com/3028586/most-innovative-companies/our-ultimate-driverless-car-report-card>>
- [15] Matthew Moore, Beverly Lu. *Autonomous Vehicles for Personal Transport: A Technology Assessment*. Social Science Research Network, June 2011. Retrieved May 15, 2016 from [http://papers.ssrn.com/sol3/papers.cfm?abstract\\_id=1865047](http://papers.ssrn.com/sol3/papers.cfm?abstract_id=1865047).
- [16] Volvo Drive Me - the self driving car in action. Retrieved May 16, 2016 from <http://www.volvocars.com/intl/About/Our-Innovation-Brands/IntelliSafe/IntelliSafe-Autopilot/Drive-Me>.
- [17] Christos Katrakazas, Mohammed Quddus, Wen-Hua Chen, Lipika Deka. *Real-time motion planning methods for autonomous on-road driving: State-of-the-art and future research directions* Transportation Research, Elseiver, 2015.
- [18] Hossein Jula, Elias B.Kosmatopoulos, and Petros A.Ioannou, Fellow, IEEE *Collision Avoidance Analysis for Lane Changing and Merging*. IEEE Transactions on Vehicular Technology, Vol. 49, No. 6 November 2000.
- [19] Stephanie Lefevre, Dizan Vasquez, Christian Laugier. *A survey on motion prediction and risk assessment for intelligent vehicles*. ROBOMECH Journal, Springer, 2014, 1 (1), pp.1.
- [20] Schubert R, Richter E, Wanielik G. *Comparison and evaluation of advanced motion models for vehicle tracking*. Proc.international conference on information fusion, 2008, pp 1–6
- [21] R. Pepy, A. Lambert, and H. Mounier. *Path planning using a dynamic vehicle model*, Information and Communication Technologies, ICTTA'06. 2nd, vol. 1. IEEE, 2006, pp. 781–786.
- [22] Katja Vogel *A comparison of headway and time to collision as safety indicators*, Accident Analysis and Prevention, 2003, pp. 427–433.
- [23] Pacejka, H. B. (2002). *Tyre and Vehice Dynamics*. Butterworth Heinemann.
- [24] Brad Schofield. *Model-based Vehicle Dynamics Control for Active Safety*, Lund University, 2008.
- [25] Lee, A.Y. *Performance of Driver-Vehicle in Aborted Lane change maneuvers*
- [26] Nosratinia, M. *ITC compatible splines for ManGen*
- [27] Mattias Bränström, *Decison- making in Automotive Collision Avoidance Systems*, Department of Signals and Systems, Chalmers University of Technology, Göteborg, Sweden 2011
- [28] Julia Nilsson, Mattias Bränström, Erik Coelingh, and Jonas Fredriksson, *Longitudinal and lateral control for automated lane change maneuvers*, 2015 American Control Conference, Palmer House Hilton, July 1-3, 2015, Chicago, IL , USA
- [29] Nikolce Murgovski and Jonas Sjöberg. *Predictive cruise control with au-*

*onomous overtaking*

[30] Bo Egardt. *Model Predictive Control*. Lecture Notes. 2015.

[31] Jan Maciejowski. *Predictive Control with constraints*. Prentice Hall 2002.

